PHILOSOPHICAL TRANSACTIONS OF THE ROYAL SOCIETY A MATHEMATICAL, PHYSICAL & ENGINEERING SCIENCES

Sound Generated Aerodynamically Revisited: Large-Scale Structures in a Turbulent Jet as a Source of Sound

R. Mankbadi and J. T. C. Liu

Phil. Trans. R. Soc. Lond. A 1984 **311**, 183-217
doi: 10.1098/rsta.1984.0024

Phil. Trans. R. Soc. Lond. A **311**, 183–217 (1984) [183]
Printed in Great Britain

SOUND GENERATED AERODYNAMICALLY REVISITED: LARGE-SCALE STRUCTURES IN A TURBULENT JET AS A SOURCE OF SOUND

By R. MANKBADI* and J. T. C. LIU

The Division of Engineering, Brown University, Providence, Rhode Island 02912, *U.S.A.*

(*Communicated by Sir James Lighthill, F.R.S. – Received* 5 *September* 1983)

CONTENTS

Lighthill's formulation of the aerodynamic sound problem (Lighthill, *Proc. R. Soc. Lond.* A **211**, 564 (1952)) is here considered as fundamental to the sound generated by real turbulent jets. For convenience, the aerodynamic sound integral is recast, via Michalke & Fuchs (*J. Fluid Mech.* **70**, 179 (1975)), into a form involving the pressure fluctuations. It is first conjectured that the large-scale coherent structures in the turbulent jet, whose existence is now well recognized, would be responsible for the spectrally dependent highly oriented radiation patterns in the aerodynamic sound field. Accordingly, only contributions that arise from the coherent structures are retained in the aerodynamic sound integral. The neglected fine-grained turbulence as far as the sound field is concerned is thought otherwise to contribute to the broad-band, nearly isotropic radiation. The present source description follows Mankbadi & Liu (*Phil. Trans. R. Soc. Lond.* A **298**, 541 (1981)), but suitably modified to include an ensemble of $n = 0$ axisymmetric and $n = 1$ spiral modes in the relevant Strouhal number range. The coherent structures interact with the mean flow and the fine-grained turbulence as an ensemble through energy exchanges dictated by rates

* Present address: Department of Mechanical and Aerospace Engineering, Rutgers University, Piscataway, New Jersey 08854, U.S.A.

according to their individual spectral characteristics. Because such coherent structures are relatively 'weak' in a real, developing turbulent jet, their mutual interactions are neglected as a first approximation. The sound sources, in a stationary coordinate system and evaluated at the appropriate retarded time, give rise to an equivalent streamwise distribution of line radiators after performance of the azimuthal and radial integrations in the aerodynamic sound integral. The streamwise oscillation of the equivalent sources is determined by an axial interference function strongly influenced by the wavenumber of each individual mode whereas the streamwise growth and decay of the source envelope is determined primarily by the coherent structure amplitude whose spectral dependence is also strong. The streamwise net imbalance of the source contribution, reflected by the axial integration in the aerodynamic sound integral, gives rise to the far sound field. It is found that in general, the radiation is primarily in the direction of the jet exhaust; the radiation patterns of the $n = 0$ modes resembling those of longitudinal quadrupoles and those of the $n = 1$ modes resembling those of lateral quadrupoles. However, the $n = 0$ modes tend to peak at Strouhal numbers less than those of the $n = 1$ modes. The superposition gives a directional-spectral behaviour that strikingly resembles that of observations: lower frequency sound radiates preferentially in the forward direction and as the frequency increases, the peak radiation moves towards the lateral directions; it is also found that contributions to the high-frequency sound come from coherent structures that peak nearer the nozzle lip, whereas contributions to the low-frequency sound come from such structures that peak further downstream in the jet. The calculated spectral shapes are narrower than observations by typically a deficit of 4–7 dB per octave on both the high and low frequency sides and this is most likely attributable to the nearly isotropic radiation caused by the broad-band fine-grained turbulence whose direct contribution to the sound field is not accounted for. For the same reason, the calculated aerodynamic sound field has a large deficit compared with observations in the vicinity of the 90-degree region. The dominant contributions to the radiation come from the so-called shear noise in the forward arc, whereas both the shear and self-noise of the coherent structures become equally insignificant to the same order in the 90-degree region. Although the source distribution within the jet is calculated for an identically incompressible fluid, it is used in a limited sense to study the effect of jet exit velocity on the peak radiation frequency in the forward direction: it is found that the peak value of fd/a_0, where f is the frequency, d the jet nozzle diameter and a_0 the ambient sound speed, take on a value of about 0.30 independently of the jet velocity and this compares favourably with an observational value of about 0.20. In general, the angular distribution of the peak frequency due to coherent structures radiation compared favourably with observations. Compressibility effects that somewhat limit the amplification of coherent structures, as well as the effects of higher azimuthal modes whose radiation would peak at higher frequencies and larger lateral directions, warrant further study in the light of the present considerations. The present work, however, has already shown that the consequences of Lighthill's formulation of the aerodynamic sound problem agree with major features of observations and that this is brought about by taking into account as sources the growing and decaying large-scale coherent eddies whose development within the turbulent jet and whose radiational properties are all strongly dependent upon their spectral contents.

1. Introduction

The physical features obtained from the earliest cold subsonic jet noise experiments (Fitzpatrick & Lee 1952; Gerrard 1953, 1956; Lassiter & Hubbard 1952; Westley & Lilley 1952) were thoroughly discussed by Lighthill (1954). These earlier experiments indicated that the acoustic power output scales very nearly as the eighth power of the jet exit velocity and that the spectrum of far-field sound is rather broad but that the peak frequencies are in a range around a Strouhal number of about 0.50 (although there were already indications then that

peak frequencies did not increase as fast as the jet exit velocity). The higher-frequency sound appeared to come from the region closer to the jet nozzle while lower-frequency sound appeared to come from regions further downstream. The far-field directional maximum for low-frequency sound lay closer to the jet axis, and as the frequency was increased the directional maximum shifted away from the jet axis but was still at an acute angle with that axis. The sound intensities closer to the jet axis increased with a higher power of the jet exit velocity than intensities at larger angles. Many of these features were confirmed by Lush (1971), who performed jet noise experiments under much better controlled conditions. Lush (1971) showed conclusively that in the region closer to the jet axis the peak frequencies did not scale as the Strouhal number $St = fd/U_e$ but were instead independent of the jet exit velocity. Away from the region near the jet axis the peak frequencies scaled as the Strouhal number. The general conclusion was that the acoustic-flow interaction process becomes important for sound nearer the jet axis. Clearly, once generated in the jet, that component of sound, whose wavelength is small compared with its distance of travel in the jet flow will be affected by acoustic-flow interaction processes.

One of the main reasons for the formulation of new acoustic analogies (Dowling *et al.* 1978; Lilley 1971; Pao 1973; Phillips 1960; Ribner 1964) directed at improving Lighthill's theory of aerodynamic sound generation (Lighthill 1952, 1954, 1962, 1963) is the criticism that Lighthill's theory cannot explain some of the major features of jet noise observations, for instance, the spectral behaviour of the sound field as a function of angular distribution from the jet axis. In fact, one of the more severe criticisms is that the Doppler frequency correction in Lighthill's convected quadrupoles gives rise to higher-frequency sound close to the jet axis and lower-frequency sound as the angle to the jet axis is increased for a given source of fixed frequency. Such comparisons, however, are based on the assumption that sources of different frequencies do not radiate sound differently; in other words, the possibility that the eddies radiate sound as frequency-dependent highly oriented quadrupoles is ruled out. The question that naturally arises, then, is whether the discrepancy between Lighthill's theory and observations occurs because of (1) the absence in Lighthill's theory of an *explicit* mechanism for the acoustic-flow interaction process or (2) an over-simple or simplistic interpretation of Lighthill's theory which ignores the issue of the actual spectral behaviour of the aerodynamic sound sources. Although it is most likely that both of the above reasons are true, one might expect that Lighthill's theory, if interpreted in a more fundamental manner, would be able to describe correctly the spectrally dependent jet noise radiation patterns except in a region very near the jet axis (a 'refraction valley' (Ribner 1977)). There the breakdown of Strouhal scaling, resulting in the peak radiation frequency becoming independent of the jet exit velocity, has been attributed to acoustic-flow interaction effects (Lush 1971). We shall show that the Strouhal scaling breakdown is obtainable from Lighthill's theory by taking into account the proper dynamical effects of the sources.

For some time now the large-scale coherent eddies in turbulent shear flows have been thought to be an efficient source of jet noise (Bishop *et al.* 1971; Liu 1971, 1974; Mollo-Christensen 1960, 1967). Study of the spatial development of such coherent eddies reveals that high-frequency eddies have a shorter streamwise lifespan and are concentrated in regions close to the nozzle lip, whereas low-frequency coherent eddies have a much larger streamwise lifespan and occur over extended regions of the shear layer or jet (Liu 1974; Merkine & Liu 1975; Alper & Liu 1978; Mankbadi & Liu 1981). Furthermore, the near pressure field and its

PHILOSOPHICAL TRANSACTIONS OF THE ROYAL SOCIETY A MATHEMATICAL, PHYSICAL & ENGINEERING SCIENCES

spectral behaviour obtained theoretically (Liu 1974; Merkine & Liu 1975) strikingly resemble those obtained from the earlier jet noise observations which indicated that the high-frequency sound sources are located in regions near the nozzle exit and low-frequency sound sources extend over large regions along the jet. There remained, then, the theoretical studies that would identify such sources with the spectral, directional behaviour of the far-field sound. This has been shown to be indeed the case in some preliminary calculations for the far sound field (Liu 1977; Liu *et al.* 1977) with Lighthill's theory (1952) for the spatially developing coherent eddies in a plane mixing layer (Alper & Liu 1978). Liu (1977) and Liu *et al.* (1977) showed that the low-frequency far-field sound, which comes from the low-frequency coherent eddies whose effective lifespan occupies a lengthy streamwise stretch along the shear layer, is pointed in a direction close to the 'jet axis'; the high-frequency far-field sound, which comes from the high-frequency eddies whose effective lifespan occupies a shorter streamwise region, is pointed away from the axis. However, the overall sound field contributed by the eddies in a plane mixing layer is like that of axisymmetric eddies in a round jet in that the radiation field behaves like a combination of streamwise-longitudinal and lateral quadrupoles and contribute very little sound in a direction normal to the jet axis. In spite of this shortcoming in explaining the behaviour of the far-field sound from a real round jet, those studies brought out the correct qualitative directional behaviour of the acoustic radiation properties of coherent eddies. More importantly, it was clear even in that much simplified treatment that the radiation patterns from different frequency coherent eddy sources are oriented differently. This effect, in fact, overwhelms the Doppler-frequency correction so as to render Lighthill's theory (applied to the plane mixing layer sources) qualitatively similar to the observations of the spectral dependence of the radiation pattern. This, then, provides the impetus for the consideration of far-field sound from the technologically important round turbulent jet. It is certainly worthwhile to put to the test the premise that Lighthill's theory (1952, 1954, 1962, 1963), when fundamentally interpreted without circumventing the issue of real jet noise sources, provides a description of the spectrally dependent jet noise radiation patterns in accord with observations except in a region close to the jet axis (where a more explicit description of acoustic-flow interaction process which is only implicitly accounted for in Lighthill's theory is necessary).

Before presenting the formulation of the problem in terms of appropriate jet noise sources, we discuss its features further. The sound of a given frequency received at a given point in the far field is a net result of the interference between the sound emitted from different regions along the streamwise lifespan of the travelling wavy coherent eddies at the same frequency. After the radial and azimuthal contributions are taken into account, the radiation properties are not unlike that of a line source with a streamwise envelope of increasing and decaying magnitude along the jet. This envelope is the result of the modification of the coherent eddy amplitude by the radial interference between the sound emitted from different radial parts of slices of the jet. However, the streamwise envelope characterizing the radiation properties reflects the actual streamwise lifespan of the eddies. That is, the envelope peaks further downstream for lower-frequency eddies and is stretched over larger streamwise distances, while the higher-frequency eddies give rise to a shorter streamwise envelope which peaks closer to the nozzle lip. The streamwise interference takes place as an oscillation under the envelope, and is contributed primarily by the streamwise travelling wavy properties of the coherent eddies. The far-field sound is the net result of such interferences. The coherent eddy contribution to

aerodynamic sound thus follow rather closely the properties of the eddies themselves of growing and decaying oscillations. As we have seen from studies of the coherent eddies, their growth in amplitude is due primarily to energy production from the mean motion and their decay is due primarily to energy transfer back to the mean flow and to the fine-grained turbulence. This growth and decay process for coherent eddies in turbulent shear flows has been the subject of intense study in terms of basic physical principles (Liu & Merkine 1976; Alper & Liu 1978; Gatski & Liu 1980), in particular, for coherent eddies in a round turbulent jet (Mankbadi & Liu 1981). Of equal importance is the nature of the oscillations under the growing and decaying envelope which are responsible for the interference effect of far-field sound cancellations. There are, in general, two apparent mechanisms responsible for the change in wavelength of the oscillations. One mechanism for the change in wavelength of the coherent eddies is the convection of such eddies of a given physical frequency into regions of varying mean flow; their convection speeds and wavelengths adjust accordingly so that these properties are very nearly scaled locally, according to observations. The other mechanism is visually describable as the agglomeration of eddies or 'pairing' observed in shear flows of moderate Reynolds number (Winant & Browand 1974). Although also present in large Reynolds number shear flow (Roshko 1976), the visual observation of pairing is less pronounced than at lower Reynolds numbers, and the main mechanism for the demise of large coherent eddies appears to be the generation of fine-grained turbulence (Dimotakis & Brown 1976). Even at moderate Reynolds numbers, the pairing events occur almost regularly in the shear layer, and their contribution to the far-field sound comes not from a single pairing event but from a net non-cancellation of the interference effect of a series of such events under a growing and decaying envelope. Caution about the interpretation of 'pairing' comes from Williams & Hama (1980). They computed streaklines for a shear layer perturbed by various linear superpositions of assumed propagating, constant amplitude fundamental and subharmonic waves and found that the streaklines gave visually an apparent amplification, possible nonlinearity and 'pairing'. These are not present in the assumed flow but attributable to wave interference. The sources of aerodynamic sound in the present work consist of the superposition of a wide spectrum of growing and decaying coherent eddy modes. The computation of streaklines from such a superposition, though not intended, could always be obtained and the visual effects of wave interference, via Williams & Hama (1980), would be recoverable. The main physical feature important to aerodynamic sound is present in that from the work of Mankbadi & Liu (1981); a fundamental mode would decay in a spatial region as its subharmonic begins to amplify so that the respective wave envelope peaks do not overlap spatially. This gradual fade-in and fade-out process, rather than an abrupt switch in modal content that might have been suggested by visual observations, is quantitatively measured by Ho & Huang (1982). An abrupt switch in modal content can, of course, generate sound (Ffowcs Williams & Kempton 1978). The peaks in the measured energy content are attributable dominantly to the coherent mode–mean flow interaction; mode–mode interactions affect only the details (Liu & Nikitopoulos 1982). Both of the mechanisms for spatial wavelength modulation as well as the spatial amplitude modulation in a real developing turbulent jet are present in the same model.

From this discussion, we see that the modelling of the aerodynamic sound source oscillations in terms of a physically derived 'switch-on' and 'switch-off' process is most crucial. The large-scale coherent eddy structure in a round turbulent jet discussed by Mankbadi & Liu (1981) furnishes the 'proper' aerodynamic sound source for the present discussion of the far-field sound.

2. Discussion of the formulation

The discovery of large-scale coherent structures in turbulent shear flows (see, for example, Brown & Roshko 1974; Roshko 1976) and the realization of the importance of such structures in the flow noise problem (Bishop *et al.* 1971; Liu 1971, 1974; Mollo-Christensen 1960, 1967) naturally leads to a new emphasis on the theoretical understanding of aerodynamic sound. Rather than taking the sound source as given by the total flow fluctuations (random and coherent), which are difficult to obtain, the sound source is considered as dominated by the organized fluctuations. Consequently, it is now possible to describe the source (Mankbadi & Liu 1981) in a manner adequate for performing the volume integration involved in Lighthill's (1952, 1962) solution. Along this line of thought, Michalke (1969) considered a train of propagating waves with amplitude that oscillated in time but uniform in the direction of propagation. He found that because of cancellations such a wave produces no sound in the far field, but that if this wave is cut off, it radiates sound that depends on the location of this cutoff. This work, however, has stimulated much of our work towards a physical (rather than arbitrary) cutoff of the large-scale structure as a consequence of its natural development in a turbulent jet. Yamamoto & Arndt (1978) also found that the far-field sound intensity is sensitive to the extent of longitudinal and lateral source distribution and hence to the cutoff mechanism. The development of large-scale coherent structure in a turbulent jet, obtained by Mankbadi & Liu (1981) from fundamental conservation principles, furnishes the aerodynamic sound sources in the present study. We consider here a round jet exhausting into still air from a nozzle of a given diameter d and nozzle exit velocity U_e which is less than the speed of sound. The jet's temperature is the same as the ambient temperature and the Reynolds number is large enough for the flow to be turbulent. The flow fluctuations are decomposed into coherent and random components. Then the sound source is taken to be dominated by the large-scale coherent structure. Thus, the volume integral in Lighthill's theory (1952) can be evaluated to study the sound produced by this large-scale structure and at the same time to test Lighthill's theory with a realistic model for the sound source, one obtained from basic principles.

To evaluate Lighthill's integral in detail with the present ideas, we note that Michalke & Fuchs (1975) took into account the geometrical configuration of a circular jet and used a cylindrical coordinate system to describe the source term in Lighthill's solution. They expanded the source term in a Fourier series with respect to the azimuthal angle and performed an azimuthal integration to obtain an expression for the shear noise in terms of the sum of the cross-spectral density of each single azimuth-frequency component of the noise source. In Michalke & Fuchs (1975), this spectral density must be measured before the remaining radial and axial integrals of Lighthill's solution can be evaluated. Their interpretation of Lighthill's theory is appropriate for the present analysis as it enables us to study the noise produced by each azimuthal mode of a given organized structure. However, since Mankbadi & Liu (1981) provide the fluctuating source term, the work of Michalke & Fuchs (1975) is modified to relate the sound intensity to known fluctuating wavelike sources rather than to yield it in terms of correlations. Further, the analysis here shows that the self-noise is small relative to the shear noise everywhere except in the vicinity of the 90° region where both contributions are weak. The sound intensity thus can be classified according to the frequency ω and the azimuthal wavenumber n of the sources in addition to the noise classification as shear and self-noise. The measurements of Yamamoto & Arndt (1978) suggest that for Strouhal numbers between 0.1 and 1.0, only the axisymmetric

and the first helical (asymmetric) modes have any practical importance in jet noise. Here we study in detail the noise produced by the axisymmetric and the asymmetric ($n = 1$) modes of the large-scale coherent structure. This can always be extended to include other higher modes.

(*a*) *The aerodynamic sound problem*

Lighthill (1952) considers a fluid in which a finite region contains an unsteady flow. Far away from that region, the fluid is at rest and uniform with density ρ_0 and sound speed a_0. By rearranging the exact equations of motion, Lighthill obtains an expression for the sound

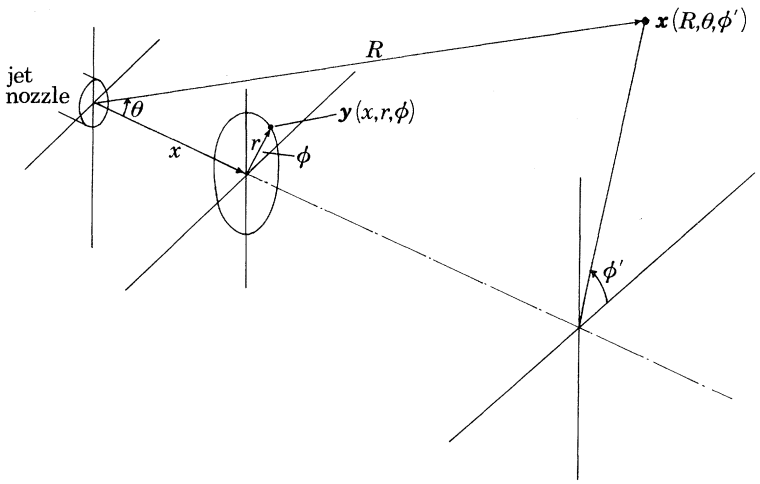

FIGURE 1. Jet coordinate system.

pressure in terms of the flow fluctuations. For flows at moderate subsonic speeds, large Reynolds number and temperatures equal to the ambient temperature, Lighthill's solution for the far-field sound reduces to

$$p_s(\boldsymbol{x}, t) = \frac{1}{4\pi R}\frac{x_i x_j}{R^2}\frac{1}{a_0^2}\int_v \mathrm{d}v\left[\frac{\partial^2}{\partial t^2}(\rho c_i c_j)\right], \tag{2.1}$$

where p_s is the sound pressure at the observation point $\boldsymbol{x}$, R is the distance from the nozzle exit to the observation point, c_i is the total flow velocity in cartesian coordinates x_i, while $\mathrm{d}v$ is the volume element of the source region. The square brackets indicate that the quantities within are evaluated at the retarded time t_r defined as

$$t_r = t - |\boldsymbol{x} - \boldsymbol{y}|/a_0, \tag{2.2}$$

where $\boldsymbol{y}$ is the location of the source inside the jet flow. In the present analysis for a circular jet, the cylindrical coordinate system is adopted to locate the source point $\boldsymbol{y} = (x, r, \phi)$, while the far-field observation point is denoted by spherical coordinates $\boldsymbol{x} = (R, \theta, \phi')$. This co-ordinate system is shown in figure 1.

Equation (2.1) can be written as

$$p_s(\boldsymbol{x}, t) = \frac{1}{4\pi R a_0^2}\int_v \mathrm{d}v\left[\frac{\partial^2}{\partial t^2}(\rho c_r^2)\right], \tag{2.3}$$

where c_r is the full velocity component in the observer's direction along R. By using the inviscid

equations of motion, Michalke & Fuchs (1975) showed that (2.3) can be transformed to the following equivalent form:

$$p_s(\boldsymbol{x}, t) = \frac{1}{4\pi R a_0^2}\int_v \mathrm{d}v\left[\frac{\partial}{\partial t}\left(f_1 p\,\frac{\partial c_r}{\partial y_r}\right)+\frac{1}{a_0}\frac{\partial^2}{\partial t^2}\left(f_2 p c_r\right)\right], \tag{2.4}$$

where $f_1 = 2/(1-M_r)^3$, $f_2 = (2-M_r)/(1-M_r)^2$ and $M_r = c_r/a_0 < 1$, $\partial/\partial y_r$ is the gradient in the R-direction and p is the flow pressure. Equation (2.4) has the advantage that the shear-noise source can be expressed in terms of a scalar quantity p rather than the non-scalar velocity. The volume integral of (2.4) is evaluated with respect to a fixed frame of reference, and the directivity factors $(1-M_r)^{-k}$ in (2.4) are obtained through introduction of the pressure p and are not the usual convection factors of the form $(1-M_c\cos\theta)^{-k}$ obtained by taking Lighthill's solution to a frame of reference moving with a convection Mach number M_c.

In order to evaluate the volume integral of (2.4) the fluctuating values of p and c_r must be known in advance. Following suggestions in work on modelling of large-scale structures in turbulent shear flows (Liu 1971, 1974; Liu & Merkine 1976; Alper & Liu 1978; Mankbadi & Liu 1981), each flow quantity g is split into three components: the steady mean flow G, the large-scale coherent structure $\tilde{g}$, and the fine-grained turbulent structure g'. Thus we set:

$$\left.\begin{aligned} c_r &= U_r+\tilde{u}_r+u_r';\\ \text{and}\qquad p &= P+\tilde{p}+p'. \end{aligned}\right\} \tag{2.5}$$

Using the discussion above, we consider here the sound generated by the coherent structure, assuming that it is more efficient than the fine-grained turbulence in emitting sound. Although the sound radiated by the fine-grained turbulence is not taken into account here, the fine-grained turbulence plays an indirect but crucial role in that it controls the development of the coherent structure and consequently its emitted sound. Upon substituting (2.5) into (2.4), neglecting terms that include p' or u_r', we obtain the following expression for the sound pressure up to second order in the disturbances

$$p_s(\boldsymbol{x}, t) = \frac{1}{4\pi R a_0^2}\int_v \mathrm{d}v\left\{\bar{f}_1\frac{\partial U_r}{\partial y_r}\left[\frac{\partial\tilde{p}}{\partial t}\right]+\bar{f}_2\bar{M}_r\left[\frac{\partial^2\tilde{p}}{\partial t^2}\right]\right\}$$

shear noise

$$+\frac{1}{4\pi R a_0^2}\int_v \mathrm{d}v\left\{\frac{3\bar{f}_1}{1-\bar{M}_r}\frac{\partial U_r}{\partial y_r}\frac{1}{a_0}\left[\frac{\partial\tilde{p}\tilde{u}_r}{\partial t}\right]+\bar{f}_1\left[\frac{\partial}{\partial t}\left(\tilde{p}\,\frac{\partial\tilde{u}_r}{\partial y_r}\right)\right]+\frac{\bar{f}_2}{a_0}\left(1+\bar{M}_r\frac{3-\bar{M}_r}{2-\bar{M}_r}\right)\left[\frac{\partial^2\tilde{p}\tilde{u}_r}{\partial t^2}\right]\right\}, \tag{2.6}$$

self-noise

where $\bar{f}_1$ and $\bar{f}_2$ are evaluated at $\bar{M}_r = U_r/a_0$.

Source terms which are first order in the coherent structure quantities can be termed first order or shear noise. Source terms which are second order in the coherent structure quantities can be termed second order or self-noise. The terminology shear and self-noise is consistent with conventional terminology. These shear and self-noise terms are equivalent to $U_i\tilde{u}_j$ and $\tilde{u}_i\tilde{u}_j$ respectively, and therefore are equivalent to Lighthill's (1952, 1954) shear and self-noise terms. In what follows, shear and self-noise will be considered separately.

(*b*) *The shear noise*

At low Mach numbers the shear noise term in (2.6) is the same shear noise discussed by Lighthill (1954), except that Lighthill neglected the second time-derivative of p on the basis that it represents an octopole field of a relatively weaker noise field. The second time-derivative

of p is kept here since it may be important at higher frequencies, as suggested by Michalke & Fuchs (1975). In the present coordinate system (figure 1) $\partial/\partial y_r$ is given by

$$\frac{\partial}{\partial y_r} = \cos\theta\frac{\partial}{\partial x}+\sin\theta\cos\Delta\frac{\partial}{\partial r}-\sin\theta\sin\Delta\frac{\partial}{r\partial\Delta}, \tag{2.7}$$

where $\Delta = \phi-\phi'$ is the azimuthal angle between the observation point $\boldsymbol{x}$ and the source point $\boldsymbol{y}$. For an axisymmetric mean flow, U_r can be written as

$$U_r = U\cos\theta+V\sin\theta\cos\Delta, \tag{2.8}$$

where U, V, W are the mean velocity components in the x, r, ϕ directions, respectively.

Upon substituting (2.7) and (2.8) into the shear noise contribution to (2.6) and the use of the continuity relation for the mean flow, we obtain

$$p_{sh}(\boldsymbol{x},t) = \frac{1}{4\pi Ra_0^2}\int dv\left\{\frac{2}{(1-\bar{M}_r)^3}\left(\cos^2\theta\frac{\partial U}{\partial x}+\tfrac{1}{2}\sin 2\theta\cos\Delta\left(\frac{\partial U}{\partial r}+\frac{\partial V}{\partial x}\right)\right.\right.$$
$$\left.\left.+\sin^2\theta\left(\cos^2\Delta\frac{\partial V}{\partial r}+\sin^2\Delta\frac{V}{r}\right)\right)\left[\frac{\partial\tilde{p}}{\partial t}\right]+\frac{\bar{M}_r(2-\bar{M}_r)}{(1-\bar{M}_r)^2}\left[\frac{\partial^2\tilde{p}}{\partial t^2}\right]\right\}. \tag{2.9}$$

Now, we consider a single azimuthal-frequency component of the large-scale structure with the wavelike pattern stated as in Mankbadi & Liu (1981):

$$\left|\begin{matrix}\tilde{u}_i(\boldsymbol{x},t)\\ \tilde{p}(\boldsymbol{x},t)\end{matrix}\right| = A(x)\left|\begin{matrix}\hat{u}_i(x,r)\\ \hat{p}(x,r)\end{matrix}\right|\exp\left(\mathrm{i}\int_0^x\alpha_r(\xi)\,d\xi-\mathrm{i}\omega t+\mathrm{i}n\phi\right)+\text{c.c.}, \tag{2.10}$$

where $A(x)$ is an amplitude function that varies along the jet, obtained from nonlinear theory, while the radial distribution is given by $\hat{u}_i(x,r)$ and $\hat{p}(x,r)$, α_r is the wavenumber corresponding to the real frequency ω, and n is the azimuthal wavenumber which is an indication of the wavelike oscillation around the centre-line of the jet ($n = 0$ represents an axisymmetric wave while $n = 1$ represents a helical wave). For a single azimuthal-frequency component, the local linear inviscid stability theory provides α_r as the eigenvalue and $\hat{u}_i$ and $\hat{p}$ as the eigenfunctions corresponding to a given ω and n. With the form of the source distribution given by (2.10), the shear noise contribution becomes, with velocities normalized by U_e, lengths by the nozzle diameter d and pressures by $\rho_0 U_e^2$:

$$p_{sh}(\boldsymbol{x},t,St,n) = -\tfrac{1}{2}\mathrm{i}\frac{St\,M^2}{R}\int dx\,r\,dr\,d\Delta[\tilde{p}]\,(A_0+A_1\cos\Delta+A_2\cos 2\Delta)+\text{c.c.}, \tag{2.11}$$

where

$$\left.\begin{aligned}A_0 &= (2\cos^2\theta-\sin^2\theta)\,(\partial U/\partial x)/(1-\bar{M}_r)^3-2\pi\mathrm{i}\,St\,MU\cos\theta(2-\bar{M}_r)/(1-\bar{M}_r)^2,\\ A_1 &= \sin 2\theta(\partial U/\partial r+\partial V/\partial x)/(1-\bar{M}_r)^3-2\pi\mathrm{i}\,St\,MV\sin\theta(2-\bar{M}_r)/(1-\bar{M}_r)^2,\\ A_2 &= \sin^2\theta(\partial V/\partial r-V/r)/(1-\bar{M}_r)^3,\end{aligned}\right\} \tag{2.11a}$$

St is Strouhal number based on the wave frequency $f = \omega/2\pi$, the jet diameter d, and the jet exit velocity U_e, $M = U_e/a_0$ and $[\tilde{p}]$ is $\tilde{p}$ evaluated at the retarded time t_r (approximated by $t_r \approx t-R/a_0+(x\cos\theta+r\sin\theta\cos\Delta)/a_0$ in dimensional form). In (2.11), the azimuthal integration is made simpler by taking

$$\bar{M}_r \approx UM\cos\theta. \tag{2.12}$$

We now rearrange $[\tilde{p}]$ into the form

$$[\tilde{p}] = A(x)\,\hat{p}(x,r)\exp(\mathrm{i}\gamma - \mathrm{i}\psi + \mathrm{i}n\Delta - \mathrm{i}\sigma\cos\Delta), \tag{2.13}$$

where
$$\gamma(x,\theta,St,M) = \int_0^x \alpha_r(\xi)\,\mathrm{d}\xi - 2\pi\,St\,Mx\cos\theta,$$
$$\sigma = 2\pi\,St\,Mr\sin\theta,$$
and
$$\psi = 2\pi\,St\,(t - MR) - n\phi'.$$

The azimuthal integration appearing in (2.11) is the same as that obtained by Michalke & Fuchs (1975), and thus (2.11) can be written as

$$p_{sh}(\boldsymbol{x},St,n) = -\tfrac{1}{2}\mathrm{i}\,\frac{St\,M^2}{R}\,\mathrm{e}^{-\mathrm{i}\psi}\int A\hat{p}\exp(\mathrm{i}\gamma)\,Z_n r\,\mathrm{d}r\,\mathrm{d}x + \text{c.c.}, \tag{2.14}$$

where
$$Z_n = \int_0^{2\pi}\exp(-\mathrm{i}\sigma\cos\Delta + \mathrm{i}n\Delta)\sum_{l=0}^{2} A_l\cos l\Delta\,\mathrm{d}\Delta$$
$$= (-\mathrm{i})^n\pi\{2A_0J_n(\sigma) + \mathrm{i}A_1[J_{n-1}(\sigma) - J_{n+1}(\sigma)] - A_2[J_{n-2}(\sigma) + J_{n+2}(\sigma)]\}$$

and $J_n(\sigma)$ is the Bessel function of the first kind of order n and argument σ.

The shear noise intensity is obtained from (2.14) as

$$I_{sh}(\boldsymbol{x},St,n) = \frac{\rho_0 M^8 a_0^3 St^2}{4R^2}\left|\int_0^\infty A(x,St,n)\exp\{\mathrm{i}\gamma(x,\theta,St,n,M)\}\,F_{sh}(x,\theta,St,n,M)\,\mathrm{d}x\right|^2, \tag{2.15}$$

where
$$F_{sh}(x,\theta,St,n,M) = \int_0^\infty \hat{p}(x,r,St,n)\,Z_n(x,r,\theta,St,M)\,r\,\mathrm{d}r.$$

The far-field sound studied here will be based on (2.15). For a given Strouhal number, $A(x)$ and the mean flow velocity gradients are obtained from the nonlinear solution for the development of the organized structure presented in Mankbadi & Liu (1981). In (2.15) $\exp(\mathrm{i}\gamma)$ and F_{sh} are the axial and radial interference functions, respectively, for the shear noise contribution.

In order to show that this formulation is similar to that of Michalke & Fuchs (1975), we obtain the spectral density W from (2.14) as

$$W_{sh}(\boldsymbol{x},St,n) = \frac{M^4St^2}{4R^2}\int \mathrm{d}x_1\int r_1\,\mathrm{d}r_1\int \mathrm{d}x_2\int r_2\,\mathrm{d}r_2\,W_{12,n}(x_1,r_1,x_2,r_2)\,Z_n^{**}$$
$$\times Z_n\exp(-2\pi\mathrm{i}\,St\,M\cos\theta(x_2 - x_1)), \tag{2.16}$$

where
$$W_{12,n}(x_1,r_1,x_2,r_2) = A(x_1)\,\hat{p}(x_1,r_1)\exp\left(\mathrm{i}\int_0^{x_1}\alpha_r\,\mathrm{d}\xi\right)A^{**}(x_2)\,\hat{p}^{**}(x_2,r_2)\exp\left(-\mathrm{i}\int_0^{x_2}\alpha_r\,\mathrm{d}\xi\right), \tag{2.17}$$

and a double asterisk denotes a complex conjugate. Equation (2.16) is identical to the formulation of Michalke & Fuchs (1975) except for $W_{12,n}$ which is interpreted differently. In Michalke & Fuchs (1975), $W_{12,n}$ is the correlation of the total fluctuations, with no differentiation between random and coherent fluctuations, while here $W_{12,n}$ is given as the correlation of the

coherent fluctuations with the random contribution neglected. The present analysis of the shear noise is thus the same as that of Michalke & Fuchs (1975) except that we consider the coherent fluctuations, obtained according to conservation principles, as the dominant sound source.

The convenience of expressing the intensity in terms of the developing pressures of the source in (2.15) is true only for the shear noise problem. The self-noise intensity, which is not considered by Michalke & Fuchs (1975), necessarily involves the vectorial quantities $\tilde{u}_r$.

(*c*) *The self-noise*

The self-noise sound pressure, which is given by the second group of terms in (2.6), is proportional to the source amplitude square, $|A|^2$. Thus, its intensity is $I_{sf} \propto |A|^4$, whereas $I_{sh} \propto |A|^2$. In this case, for an initial flat spectrum $|A|_0^2 \approx 10^{-5}$ then I_{sf} is approximately 50 dB below I_{sh} in general, except in the vicinity of $\theta \approx 90°$ when both I_{sh} and I_{sf} are of the same order but are equally unimportant relative to the forward radiation region. Numerical computations confirm this. Consequently, the details of the self-noise are omitted here.

(*d*) *The aerodynamic sound source*

The aerodynamic sound problem formulated has taken into account sources in terms of the large-scale *coherent* structures in a round jet, in the form of (2.10) for each mode, regardless of whether such structures are developing in a laminar jet, a fully turbulent jet or a laminar jet undergoing transition. The distinction comes *primarily* through the streamwise development of the amplitude $A(x)$, which determines the envelope under which the aerodynamic sound source makes positive and negative contributions. The resulting delicate net imbalance gives rise to the far-field sound. The determination of $A(x)$ as well as the elucidation of the physical understanding of its development in a fully turbulent jet is described in Mankbadi & Liu (1981). Although applications to a variety of Strouhal number modes were made for both the axisymmetric ($n = 0$) and the first helical modes ($n = 1$), for simplicity, only a single mode at a time was considered to develop in the turbulent jet.

For a 'natural' turbulent jet, it is expected that a 'spectrum' of coherent structures is present. The immediate modifications expected would be that, in this case, the numerous modes are now sharing their respective energy exchange mechanism with the mean flow. Thus, each mode is now able to extract less energy from the mean flow compared with the single mode situation of Mankbadi & Liu (1981). This, in turn, would modify the mean jet-spreading rate as well as the energy transfer to the fine-grained turbulence. The various modes can still be considered mutually non-interacting to a first approximation compared with mode–mean flow and mode–fine-grained turbulence interactions. This is because the mode–mode interactions (which are dominated by binary interactions because of amplitude scaling) in terms of energy transfer arising from the product of a stress and rate of strain, scales as the mode amplitude to the third power. Whereas mode–mean flow interactions scale as an amplitude to the second power and the mode–turbulence interactions scale as the product of the mean fine-grained turbulence energy and mode amplitude to the second power.

For the simultaneous presence of a spectrum of coherent modes, the conditional or phase averaging is taken with respect to the lowest frequency mode. This separates the entire spectrum of coherent signals from the fine-grained turbulence. Appropriate time-averaged kinetic equations for the coherent modes, with further appropriate phase-averaging for each mode

then follow; the integrated form of which is the basis of the amplitude equations of the coherent modes. The dominant nonlinear coupling accounted for, following the previous discussions, is through the energy exchange with the mean flow and with the fine-grained turbulence. The formulation is otherwise identical to Mankbadi & Liu (1981). The integrated energy equations reduce to the following form:

mean flow

$$\frac{1}{2}\frac{\mathrm{d}}{\mathrm{d}x} I_1(\bar{\theta}) = -I'_{\mathrm{R.s.}}(\bar{\theta})\, E - \sum_{i=1}^{N} \tilde{I}_{\mathrm{R.s.}}(\bar{\theta}; St_i, n)\, |A_i|^2; \tag{2.18}$$

coherent large-scale structure

$$\frac{\mathrm{d}}{\mathrm{d}x}\left[I_2(\bar{\theta}; St_i, n)\, |A_i|^2\right] = \tilde{I}_{\mathrm{R.s.}}(\bar{\theta}; St_i, n)\, |A_i|^2 - I_{\mathrm{w.t.}}(\bar{\theta}; St_i, n)\, |A_i|^2 E \quad (i = 1, 2, \ldots, N); \tag{2.19}$$

fine-grained turbulence

$$\frac{\mathrm{d}}{\mathrm{d}x}\left[I_3(\bar{\theta})\, E\right] = I'_{\mathrm{R.s.}}(\bar{\theta})\, E + \sum_{i=1}^{N} I_{\mathrm{w.t.}}(\bar{\theta}; St_i, n)\, |A_i|^2 E - I_\epsilon(\bar{\theta})\, E^{\frac{3}{2}}. \tag{2.20}$$

The notation used and the definition of integrals is the same as that of Mankbadi & Liu (1981), except that we have here used $\bar{\theta}$ to denote the local momentum thickness so as not to confuse it with the radiation angle of the aerodynamic sound problem. We shall describe the physical meaning of the various terms in (2.18)–(2.20) but not repeat their explicit definitions (see Mankbadi & Liu 1981). The mean flow energy advection integral is $I_1(\bar{\theta})$ and (2.18) is actually an equation for the streamwise development of $\bar{\theta}(x)$ with $\mathrm{d}I_1(\bar{\theta})/\mathrm{d}\bar{\theta} < 0$. Thus $\bar{\theta}$ will grow as long as energy is extracted from the mean flow by the fluctuations: $I'_{\mathrm{R.s.}}(\bar{\theta})$ is the production integral of the fine-grained turbulence, E is the energy content of the fine-grained turbulence over a disc section across the jet; $\tilde{I}_{\mathrm{R.s}}(\bar{\theta}; St_i, n)$ is the production integral of the coherent structure corresponding to the ith frequency mode indicated by the previously defined ith Strouhal number $St_i = f_i d/U_e$ and the nth azimuthal mode number, A_i is the corresponding complex mode amplitude with the local eigenfunctions (see (2.10)) given by the local linear stability theory so normalized as to make $|A_i|^2$ the local energy content of the coherent structure across a section of the jet. In (2.19), $I_2(\bar{\theta}; St_i, n)$ is the ith coherent structure energy advection integral, $I_{\mathrm{w.t.}}(\bar{\theta}; St_i, n)$ is the ith coherent structure-turbulence energy exchange integral. In (2.20), $I_3(\bar{\theta})$ is the fine-grained turbulence energy advection integral and $I_\epsilon(\bar{\theta})$ is its viscous dissipation integral. The sum over N coherent modes in (2.18) and (2.20) reflects, respectively, the collective energy exchange between the N coherent modes with the mean flow and with the fine-grained turbulence. Equation (2.19) is N simultaneous equations for the N number of mode energies $|A_i|^2$. As discussed previously, effects to order $|A_i|^2|A_j|$ $(j \neq i)$, reflecting mode–mode interactions, have been neglected to a first approximation. The initial conditions to (2.18)–(2.20) are $\bar{\theta}(0) = \bar{\theta}_0$, $|A_i(0)|^2 = |A_i|_0^2$ and $E(0) = E_0$.

The physical understanding of the development of single modes at various Strouhal numbers is thoroughly discussed in Mankbadi & Liu (1981), including the role played by the $n = 0$ and 1 azimuthal modes. We shall present here the source development along the jet to illustrate the contrast between a spectrum of modes and that of a single mode. The Strouhal numbers here span the practical range 0.02–1.6 for $n = 0$ and 1. The simultaneous development of the amplitude $A(x)$ of the spectral components is shown in figure 2. The initial conditions consisted of a broad-band 'flat spectrum' at the nozzle exit in which the amplitude of all the

spectral components have the same value $|A|_0^2 = 10^{-5}$, corresponding to a root-mean-square (r.m.s.) velocity of about 0.3% and the fine-grained turbulence axial r.m.s. velocity is taken to be 1% of the jet exit velocity, the jet nozzle exit momentum thickness is taken to be $\bar{\theta}_0 = 0.017$ or 1.7% of the nozzle exit diameter.

These conditions are representative of 'natural' or weakly forced jets, such as those in Moore's (1977) experiments.

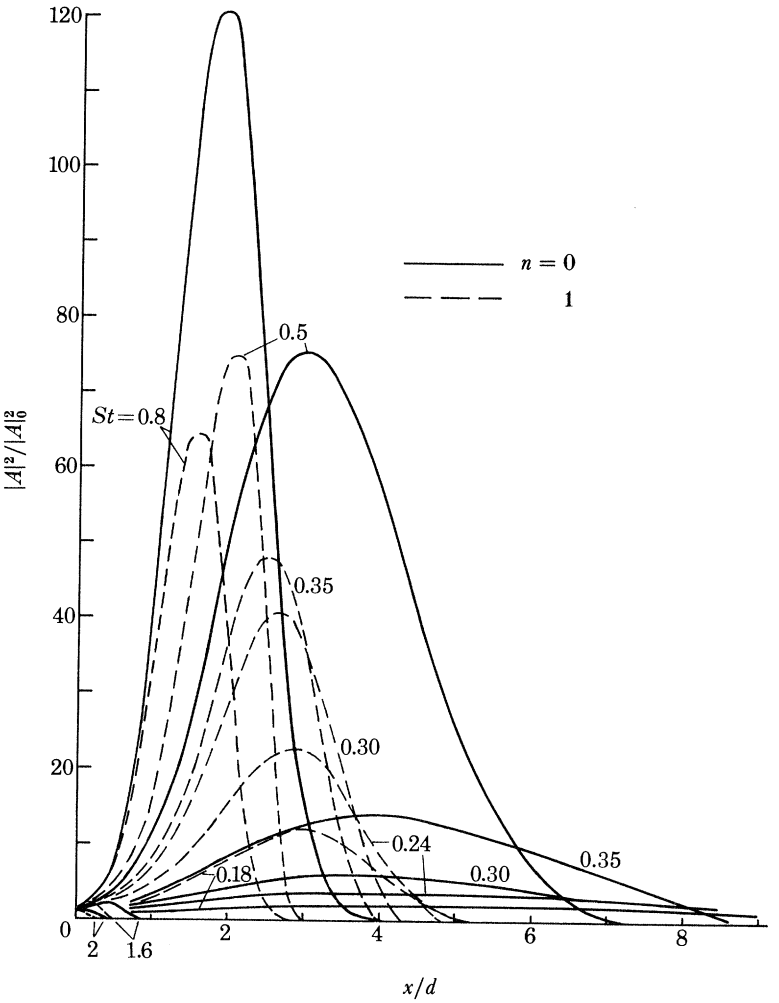

FIGURE 2. Ensemble of large-scale coherent structure amplitudes in a turbulent jet.

The streamwise development of a given mode in the spectral ensemble case is shown in figure 3 in contrast to the development of a single mode for the same initial conditions. Because the spectral ensemble now shares the production of energy from the same mean flow, the energy supply to a particular mode is now limited. Thus the amplitude or energy in this case is considerably less than the case of a single mode developing along the jet.

As has been pointed out much earlier (Liu 1974), the streamwise lifetime or extension of the source is much longer for lower Strouhal numbers and the peak amplitudes occur further downstream. We will be able to anticipate that the aerodynamic sound field of lower frequency comes from sources further downstream and that higher frequency sound from regions closer

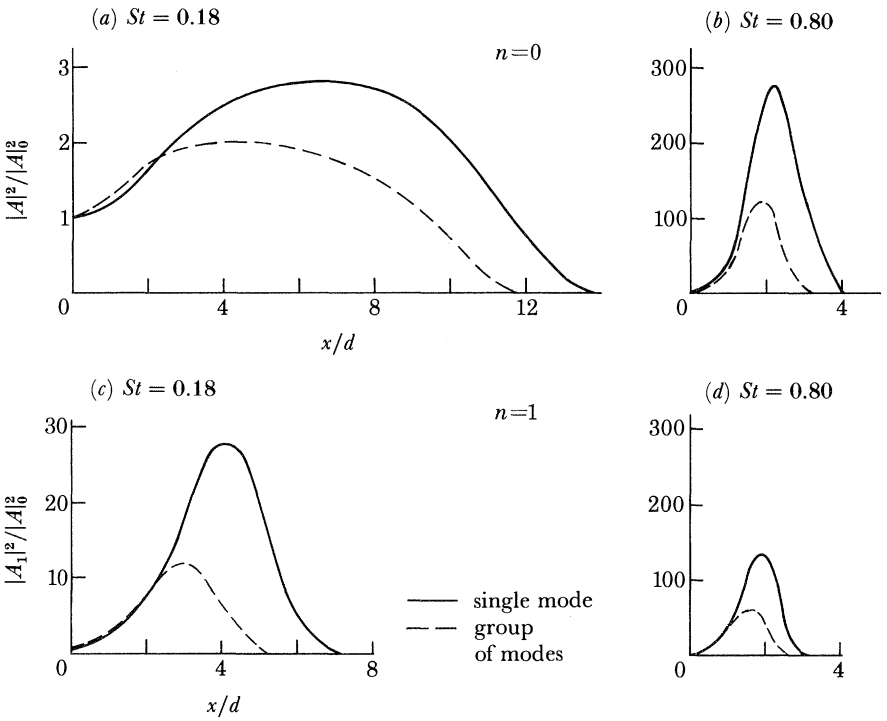

FIGURE 3. Coherent structures development in a turbulent jet. Comparison between single mode and ensemble of modes.

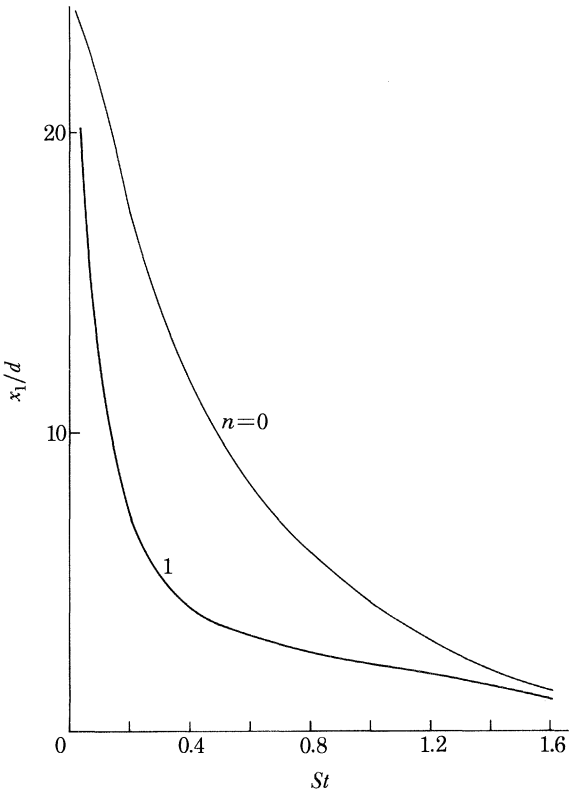

FIGURE 4. Streamwise lifespan of coherent structures.

PHILOSOPHICAL TRANSACTIONS OF THE ROYAL SOCIETY A MATHEMATICAL, PHYSICAL & ENGINEERING SCIENCES

to the nozzle lip. For the computations of the sound field, it is more convenient to rescale the streamwise source distribution in terms of a Strouhal number-dependent streamwise length scale x_1 depicting the streamwise lifetime of the source. Thus, we define x_1 such that $|A_i(x_1)|^2/|A|_0^2 = 10^{-4}$ for the ith mode. The source amplitude for the ith mode will also be correspondingly normalized by its peak amplitude $|A_i|_p$, which is also Strouhal number dependent. In the normalized case, both the amplitude and streamwise variable would be of order unity. The normalization quantities are shown in figures 4 and 5 for both $n = 0$ and 1 modes. Because, in general, the nonlinear interactions (2.18)–(2.20) are dependent on initial conditions in the region of interest, x_1 and $|A_i|_p$ are consequently also dependent on initial conditions.

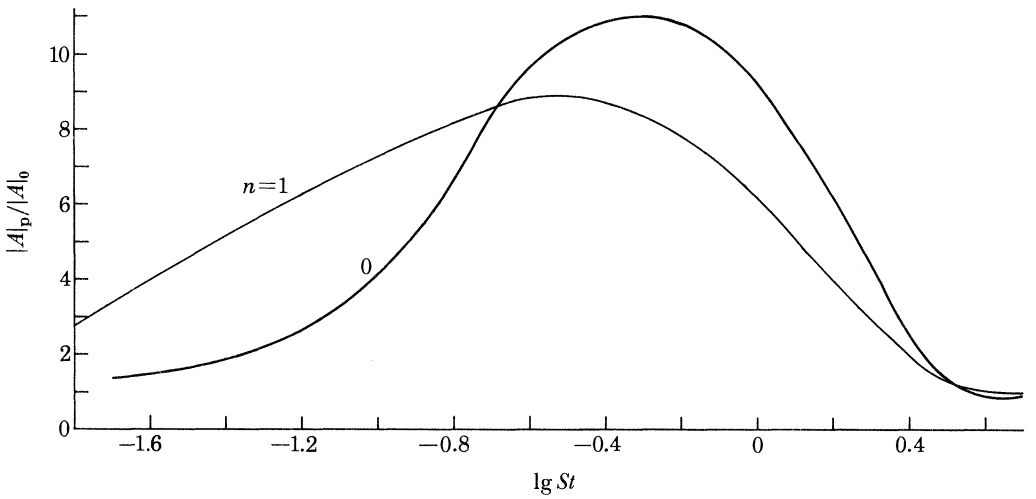

FIGURE 5. Maximum amplification of coherent structures.

The coupling between coherent structures and fine-grained turbulence in developing free turbulent flows is given much further discussion in Liu (1981). This coupling is also well demonstrated in the acoustic field (Bechert & Pfizenmaier 1975).

3. The mechanism of source contributions to the aerodynamic sound field

In Mankbadi & Liu (1981) and in the previous section, the development of the large-scale structure in a round turbulent jet for an incompressible fluid is described. The use of such a zero-Mach-number source distribution to study jet noise at subsonic speeds is justified in part not only by its simplicity, but also by observations such as those of Armstrong *et al.* (1977) which showed that the structure of turbulent pressure fluctuations varies only slightly with the Mach number. An incompressible source distribution is also consistent with the simplified sources in Lighthill's (1952, 1954) aerodynamic sound formulation discussed in §2. In this case, the large-scale coherent structures, and hence the present noise sources, depend on the Strouhal number St and the azimuthal mode number n. The observation distance R is taken as $120d$, in order to correspond to Lush's (1971) data. From the discussion in §2, we see that the observation angle from the jet axis θ is not separable from the interference functions such

as γ and $F_{\rm sh}$. These functions must therefore be evaluated for each θ before the integration along the jet axis in the acoustic output integral (2.15) can be carried out.

(*a*) *The axisymmetric* ($n = 0$) *mode*

For the $n = 0$ mode, we shall denote the interference function by $F_{\rm sh}(x, \theta, St, 0, M)$ and the contribution to the acoustic intensity by $I_{\rm sh}(R, \theta, St, 0, M)$. The latter is obtained from (2.15).

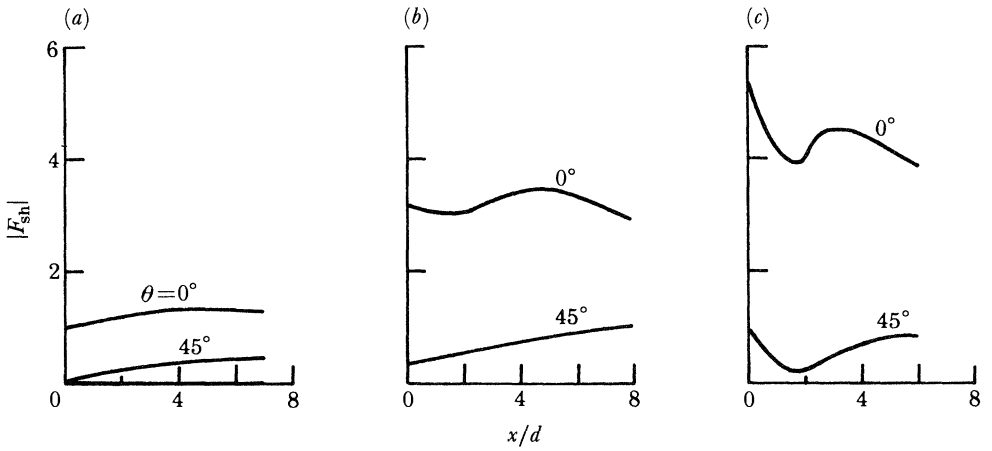

FIGURE 6. The distribution of $|F_{\rm sh}|$ along the jet for several emission angles for the $n = 0$ mode. (*a*) $St = 0.24$; (*b*) $St = 0.50$; (*c*) $St = 0.80$.

The calculated axial distribution of the shear noise radial interference function $|F_{\rm sh}(x, \theta, St, 0, M)|$ is shown in figure 6 for various Strouhal numbers and observation angles θ. The directional nature of $|F_{\rm sh}|$ is rather striking. Although it varies weakly along the jet, it decreases rapidly as θ increases, and the manner in which this takes place is strongly dependent upon the Strouhal number. In order qualitatively to explain the behaviour of $|F_{\rm sh}|$ in figure 6, approximations to $F_{\rm sh}$ will be obtained. We expand $J_l(\sigma)$ in powers of σ, assuming σ to be small. Since $\sigma = 2\pi\, St\, Mr \sin\theta$, and since the radial extent of the jet is $r \leqslant 2$, small σ is equivalent to $\theta \to 0$, π or small $(St\, M)$. Small $(St\, M)$ is in turn equivalent to either small M (since $St < 2.0$), or to low frequencies ω. Keeping terms up to the first order in $(St\, M)$, we obtain an approximate expression for $F_{\rm sh}$ as

$$F_{\rm sh}(x, \theta, St, 0, M) \approx 2\pi \int_0^\infty \frac{\hat{p}}{N^3} \left[(2\cos^2\theta - \sin^2\theta) \frac{\partial U}{\partial x} - 2\pi i\, St\, Mr \cos\theta \sin^2\theta \frac{\partial U}{\partial r} - 2\pi i\, St\, M \cos\theta N(1+N)\, U \right] r\, dr, \quad (3.1)$$

where

$$N = 1 - U(x, r)\, M \cos\theta.$$

The first and second terms in (3.1) are produced by $\partial\tilde{p}/\partial t$ in (2.6). The third term in (3.1) is produced by $\partial^2\tilde{p}/\partial t^2$ in (2.6) and was identified by Lighthill (1954) as an octopole of negligible radiation at low Mach numbers. At low Mach numbers and low Strouhal numbers, or for $\theta \approx 90°$, the first term in (3.1) is the dominant one. However, for large $(St\, M)$ and for $\theta \neq 90°$, both the second and third terms in (3.1) are significant. Thus, for a given Mach number, $\partial^2\tilde{p}/\partial t^2$ is as important as $\partial\tilde{p}/\partial t$ for aerodynamic sound at high frequencies.

For a jet flow, $\partial U/\partial x$ is small compared with $\partial U/\partial r$, and only the second and third terms in (3.1) are of importance for $\theta \neq 90°$, $St \neq 0$ and $M \neq 0$. In this case

$$F_{\rm sh} \approx -4\pi^2\, St\, M \cos\theta \int_0^\infty \frac{\hat{\rho}}{N^3}\left[U(1+N)\,N + \sin^2\theta \frac{\partial U}{\partial r} r\right] r\,{\rm d}r. \tag{3.2}$$

However, at $\theta = 90°$ only $\partial U/\partial x$ contributes to the acoustic output and therefore $F_{\rm sh}$ is very small at this angle. As (3.2) shows, $F_{\rm sh}$ is proportional to St and the integrand is also dependent on St; this explains how $|F_{\rm sh}|$ is an increasing function of St, as figure 6 shows.

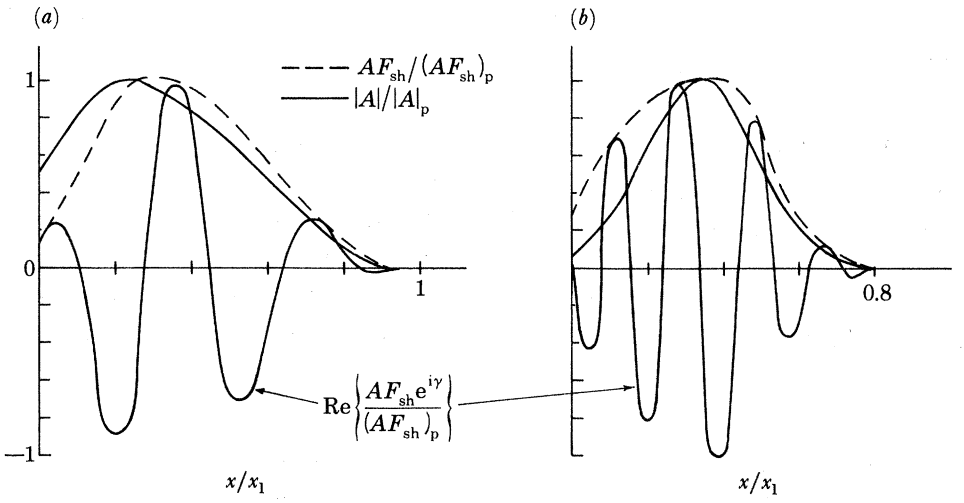

FIGURE 7. The distribution of normalized $|A|$, $|AF_{\rm sh}|$ and Re $(AF_{\rm sh} \exp {\rm i}\gamma)$ along the jet for $n = 0$, $\theta = 45°$. (*a*) $St = 0.24$; (*b*) $St = 0.80$.

The function $F_{\rm sh}$ can also be considered as the source efficiency function, since it modifies the amplitude of the sound source. The effective amplitude of the sound source is not $|A|$, but $|AF_{\rm sh}|$, as shown in figure 7 for two Strouhal numbers. We note here that high St sources are confined near to the nozzle lip whereas low St sources are stretched to encompass a larger axial distribution, in accordance with observations. However, it is plotted in figure 7 with x normalized by x_1 and $|A(x)|$ by $|A|_{\rm p}$, where x_1 is the value of x when $|A(x)|^2/|A(0)|^2 = 10^{-4}$, which reasonably indicates the streamwise lifespan of a particular large-scale component (see figure 4.) The function $|AF_{\rm sh}|$ is normalized by its value when $|A| = |A|_{\rm p}$ in figure 7.

The axial interference function appearing in (2.15), exp (iγ), plays a crucial role in the sound generation mechanism. The calculated axial variation of $AF_{\rm sh}$ exp (iγ) is shown in figure 7. It is very nearly periodic in x/d and the high-frequency components have shorter periods, as shown. The lack of exact periodicity in x/d is due to the convection of the coherent structure into regions of non-uniform mean flow. Figure 7 essentially shows the axial distribution of effective line radiators with amplitudes and wavelengths strongly influenced by Strouhal number-dependent characteristics of the large-scale structure.

We shall obtain a qualitative description of exp (iγ), in order to understand its role. We use the definition of γ given earlier to approximate it as

$$\gamma = \bar{\gamma} x, \tag{3.3}$$

where $\gamma = \bar{\alpha}_{\rm r}(1 - \bar{C}/a_0 \cos\theta)$, $\bar{\alpha}_{\rm r}$ is the average of $\alpha_{\rm r}$ over $0 < \xi < x$ and $\bar{C} = \omega/\bar{\alpha}_{\rm r}$ is the phase speed. Equation (3.3) is given here only for the sake of discussion; the results of the

calculations shown in figure 7 were performed with the full γ. The oscillatory behaviour of $\exp(\mathrm{i}\bar{\gamma}x)$ tends to convert some of the sound sources along the jet effectively into acoustic sinks, as shown in figure 7. Therefore, the sound heard in the far field is only what is left after cancellations. To assess further the role of this cancellation function, let us consider a source that has a longitudinal distribution of the form

$$AF_{\mathrm{sh}} \approx \exp\left(-(x-k\pi/\bar{\gamma})^2/c_1\right) \quad \text{for} \quad 0 < x < 2\pi k/\bar{\gamma},$$

where $k = 0, \pm 1, \pm 2, \ldots$. The presence of such an $\exp(\mathrm{i}\gamma x)$ term in the acoustic output integral (2.15) would cause the far field sound to be identically zero because of the complete cancellations. Another feature of (2.15) associated with the presence of $\exp(\mathrm{i}\gamma x)$ is that it can be written as

$$I_{\mathrm{sh}} \approx \int_0^\infty \exp(\mathrm{i}\bar{\gamma}x)\left(\frac{\mathrm{d}(AF_{\mathrm{sh}})}{\mathrm{d}x}\right)\mathrm{d}x, \tag{3.4}$$

which indicates that the sound is generated by the axial *variations* of the source along the jet. Thus, a source of a uniform amplitude produces no sound in the far field except for the switch-on or switch-off process (which may be artificial). In addition to the cancellation effect produced by $\exp(\mathrm{i}\bar{\gamma}x)$, (3.4) reveals a second cancellation mechanism. In the growing part of the wave, $\mathrm{d}(AF_{\mathrm{sh}})/\mathrm{d}x > 0$, while in the decaying part of the wave, $\mathrm{d}(AF_{\mathrm{sh}})/\mathrm{d}x < 0$. Thus the sound generated by the decaying region cancels some of the sound generated by the growth region and the far-field sound is the net imbalance.

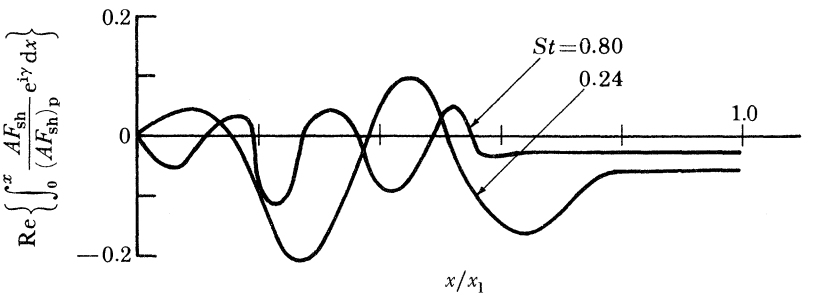

FIGURE 8. The distribution of the normalized integral $\mathrm{Re}\left(\int_0^x A(x)\, F_{\mathrm{sh}} \exp(\mathrm{i}\gamma)\,\mathrm{d}\xi\right)$ along the jet for $n = 0$, $\theta = 45°$.

The actual calculated variation of the sound source in figure 7 shows that the axial variation is neither symmetrical in effective amplitude nor uniform in effective wavelength. Axial integration of the source region must continue until the source has fully decayed to obtain the steady value of the acoustic output integral. The variations of this integral are shown in figure 8. The emphasis here is that the correct physical processes involved in the sound source $AF_{\mathrm{sh}}\,\mathrm{e}^{\mathrm{i}\gamma}$ rather than *ad hoc* estimates, are crucial to determining the acoustic output. An arbitrary cut-off of the axial integration before the steady value is reached would give an aerodynamic sound field which is also arbitrary, as pointed out earlier by Liu (1974).

The directivity of the sound intensity obtained from (2.15) is shown in figure 9 for several Strouhal numbers. This directivity is implied in both $\mathrm{e}^{\mathrm{i}\gamma}$ and F_{sh}, as we have already discussed. Since α_{r} is positive for convection in the flow direction, γ increases with θ for a fixed frequency. Hence, the cancellation effect is minimum at $\theta = 0$ and maximum at $\theta = \pi$. Thus $\mathrm{e}^{\mathrm{i}\gamma}$ tends to enhance the forward emission and to reduce the backward emission. Now F_{sh} is inversely proportional to $(1 - UM\cos\theta)^k$ which increases with θ. Therefore, F_{sh} is larger for smaller θ.

Thus, the factors of $(1 - UM\cos\theta)^{-k}$ in F_{sh} and the cancellation effect of $e^{i\gamma}$ tend to increase the forward emission and to reduce the backward emission. For this preferred forward emission, and because $F_{sh} \propto \cos\theta$, the shear noise of the $n = 0$ mode peaks at $\theta = 0°$. At $\theta = 90°$, F_{sh} is proportional to $\partial U/\partial x$, which is small for the jet flows. Therefore, the 90° shear noise of the axisymmetric wave is very small, as figure 9 shows. Thus I_{sh} for the $n = 0$ mode strongly resembles a forward longitudinal quadrupole.

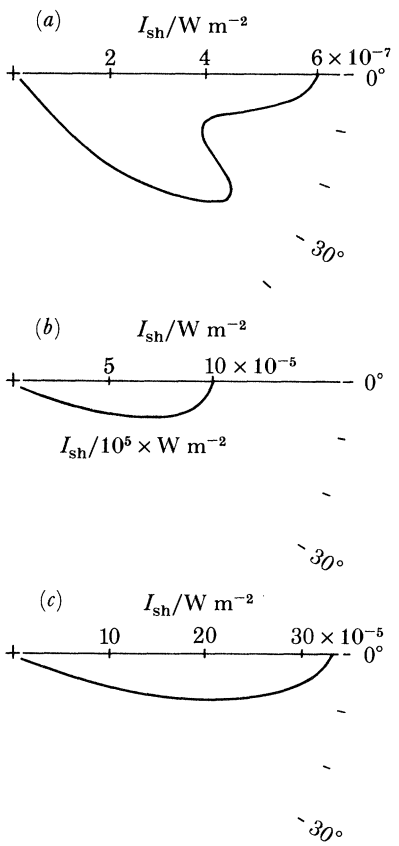

FIGURE 9. Polar distribution of the shear noise intensity I_{sh} for $n = 0$.
(*a*) $St = 0.18$; (*b*) $St = 0.30$; (*c*) $St = 0.80$.

The spectra of the sound intensity calculated according to (2.15) are shown in figure 10 for several values of θ. Acoustic intensities in decibels, dB, are referred to 10^{-12} W m^{-2}. The spectra of figure 10 are obtained by taking an initial broad band $|A|_0^2 = 10^{-5}$ for all Strouhal numbers considered. To discuss the spectral properties, (2.15) can be written as:

$$I_{sh} \approx St^2 H(St),$$

where H is a function representing the variation of the integrated sources with St. Thus H represents the dependence of A, γ, and F_{sh} on St. The amplitude $A(x)$ increases with Strouhal number until it reaches its peak amplification at $St = 0.50$–0.80, depending on the level of excitation; then its amplification reduces with further increase in St. The interference functions γ and F_{sh} are very nearly directly proportional to St. But at $\theta = 90°$, F_{sh} is independent of St. Thus $H(St)$ depends strongly on St, and therefore we cannot conclude here that the shear

noise is simply proportional to St^2 (or ω^2). Because of the nontrivial dependence of I_{sh} on St, the sound intensity first increases with Strouhal number. As the Strouhal number continues to increase, the amplification of $A(x)$ and its streamwise lifespan are reduced. In addition, γ increases proportionally to St, thereby producing strong cancellation effects. For these reasons the contribution to the sound intensity here reaches its maximum at about $St = 0.50$–0.80 then gradually decreases with further increase in Strouhal number.

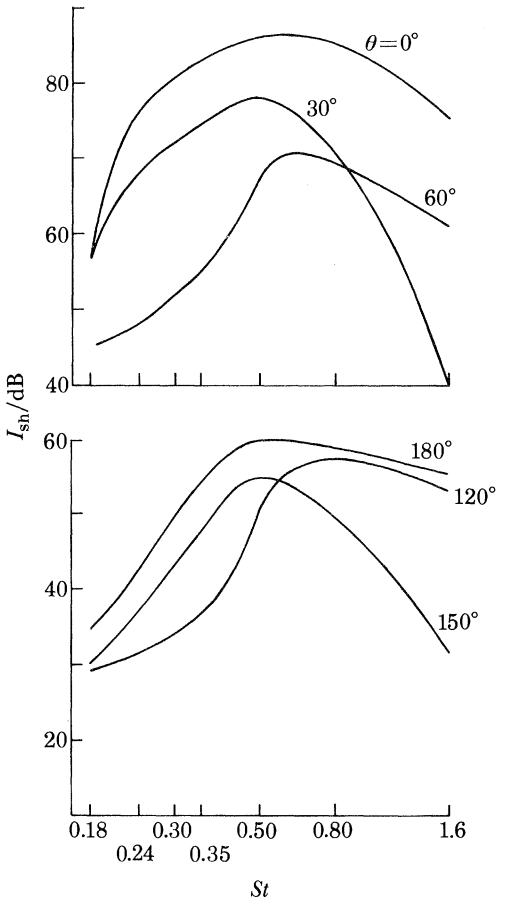

FIGURE 10. Spectra of shear noise intensity I_{sh} referred to 10^{-12} W m^{-2} for $n = 0$.

In studying the dependence of the sound intensity on the jet exit velocity we consider the sound sources to be the same as those calculated by assuming low subsonic velocities. Equation (2.15) shows that the sound intensity is an increasing function of M. It is shown in figure 11 that at small angles to the jet axis, $\theta = 15°$, the peak Strouhal number, St_p, decreases with increasing jet exit velocity, U_e. At large angles to the jet axis, $\theta = 45°$, the variation of St_p with U_e is less pronounced. The dependence on the jet velocity varies with θ, however. In the acoustic output integral of (2.15), the Mach number appears as $M\cos\theta$ in γ and also appears in the directivity factor N in F_{sh}. The dependency on Mach number is thus stronger at smaller angles to the jet axis, as figure 12 shows.

We shall delay discussion of the implications of the present calculations with respect to observations to §4 below, after a composite picture of the various contributing mechanisms has been given in what remains of the present section.

(*b*) *The first helical* ($n = 1$) *mode*

The interference functions and acoustic intensity for the $n = 1$ mode are again obtained from (2.15) and (2.22). The same initial conditions used for the source distribution in §3(*a*) are used here.

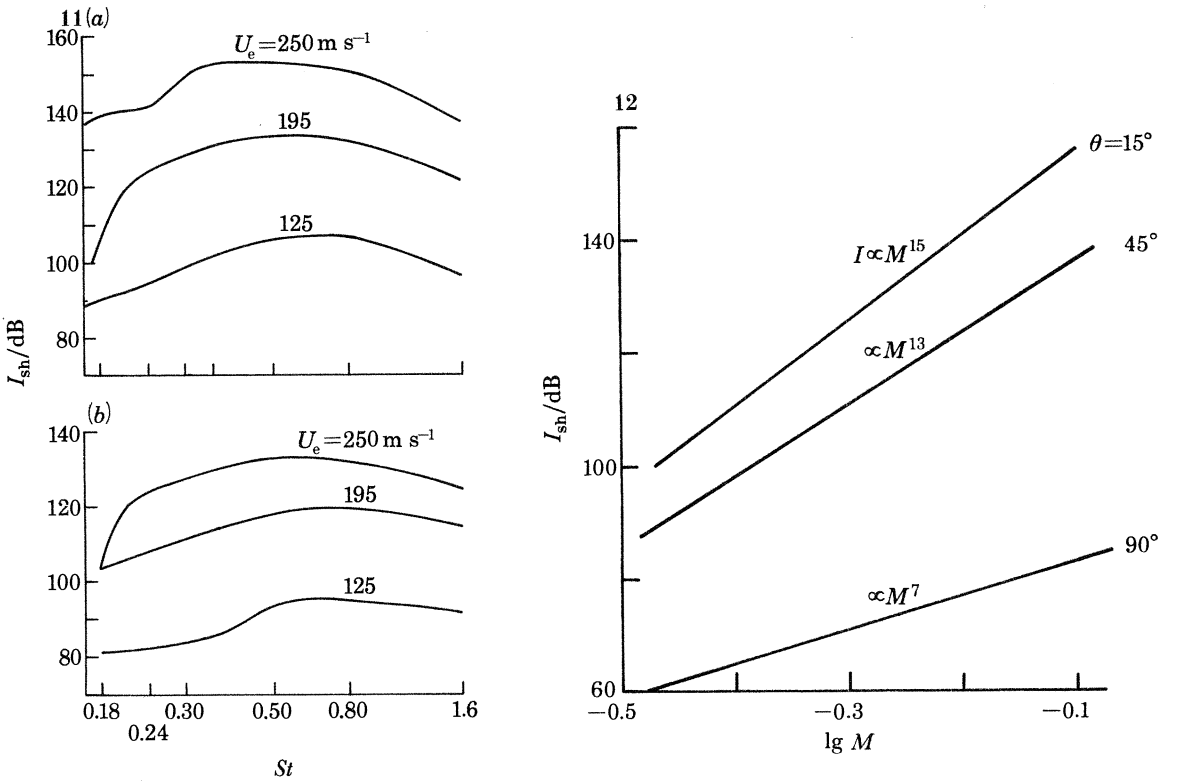

FIGURE 11. The effect of jet exit velocity on the spectra of shear noise for $n = 0$. (*a*) $\theta = 15°$; (*b*) $\theta = 45°$.

FIGURE 12. The dependence of shear noise intensity on jet exit velocity for several emission angles, for $n = 0$ and $St = 0.50$.

The distribution of the interference function $F_{sh}(x, \theta, St, 1, M)$ along the jet is shown in figure 13 for several values of St and θ. The function F_{sh} is identically zero at $\theta = 0$ and π. This is because at $\theta = 0$ or π, $J_l(0) = 0$ (except for $l = 0$, where $J_0(0) = 1$ and (2.11*a*) shows that A_1 is also zero). In order qualitatively to discuss the behaviour of F_{sh} at other angles, we again expand $J_l(\sigma)$ and retain terms up to the first order in $(M\,St)$. Hence

$$F_{sh}(x, \theta, St, 1, M) \approx \pi \int_0^\infty \frac{r\,dr\,\hat{p}}{N^3} \left\{ \sin 2\theta \frac{\partial U}{\partial r} - \pi i\, St\, M \sin\theta r \right.$$
$$\left. \times \left[\frac{\partial V}{\partial r} (4\cos^2\theta - \sin^2\theta) + V(N(1+N) + (4\cos^2\theta - 3\sin^2\theta)) \right] \right\}. \quad (3.5)$$

Equation (3.5) shows that at $\theta = 90°$, F_{sh} is given in terms of V and $\partial V/\partial r$, which are both small for the jet flows. Consequently F_{sh} is small at $\theta = 90°$. For the jet flow, $\partial U/\partial r$ is larger than V or $\partial V/\partial r$; therefore F_{sh} is approximately proportional to $\sin 2\theta$ which has a maximum at $\theta = 45°$. But because N^{-3} in (3.5) has a peak at $\theta = 0°$, F_{sh} reaches its maximum within

$0° < \theta < 45°$, although the exact angle at which F_{sh} is maximum varies with Strouhal number and Mach number. By comparing figure 13 with figure 6 it appears that

$$F_{sh}(x, \theta, St, 0, M) > F_{sh}(x, \theta, St, 1, M);$$

this indicates that the axisymmetric wave components are more efficient in emitting sound than the asymmetric ones, as was also concluded by Michalke & Fuchs (1975). The axial interference function γ is weakly dependent upon n, and therefore the role of the cancellation

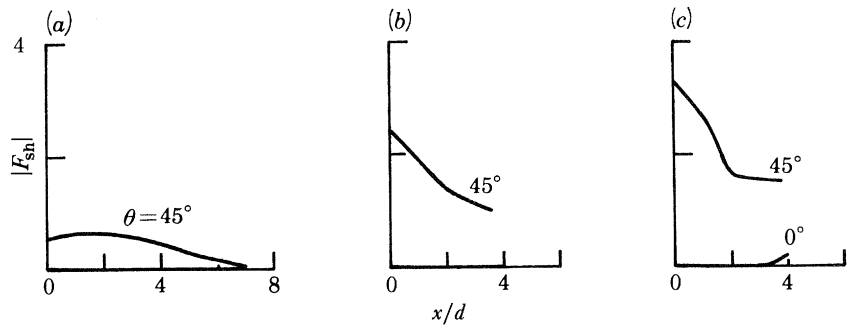

FIGURE 13. The distribution of $|F_{sh}|$ along the jet for several emission angles for $n = 1$. (*a*) $St = 0.24$; (*b*) $St = 0.50$; (*c*) $St = 0.80$.

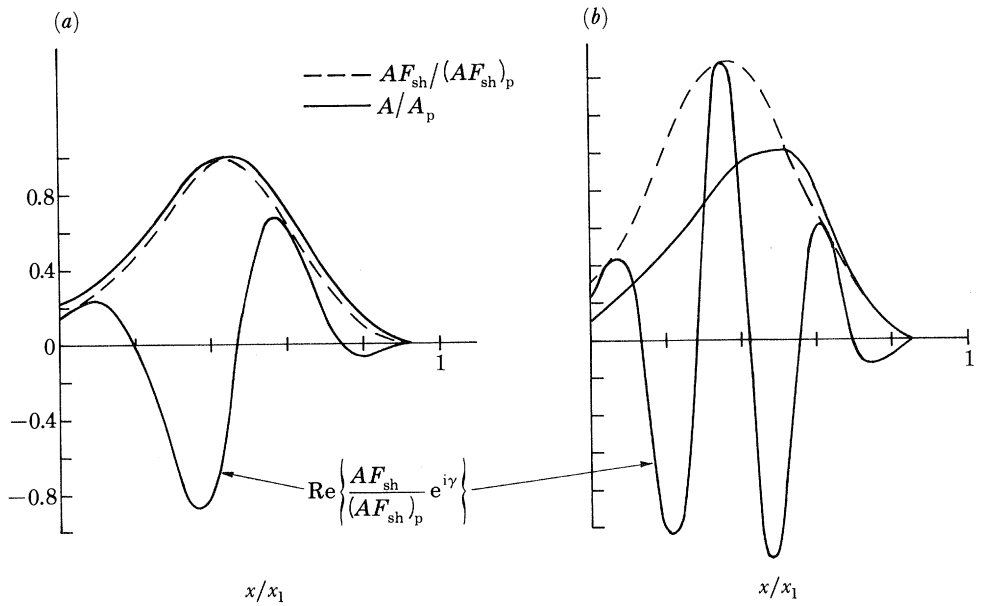

FIGURE 14. The distribution of normalized $|A|$, $|AF_{sh}|$ and Re $(AF_{sh} \exp i\gamma)$ along the jet for $n = 1$, $\theta = 45°$. (*a*) $St = 0.24$; (*b*) $St = 0.80$.

function exp (iγ) for the asymmetric mode, shown in figure 14, is quite similar to that for the axisymmetric mode shown in figure 7. The amplitude $A(x, St, 1)$ is different from $A(x, St, 0)$ in the sense that the former decays much more quickly than the latter. The extent of the source distribution along the jet shrinks as n increases from 0 to 1.

Figure 15 shows the directivity patterns of the sound intensity calculated according to (2.15). Because the cancellation effect is minimum at $\theta = 0°$ and because of the directivity factors

N^{-3} in F_{sh}, the sound emission is enhanced in the forward direction and reduced in the backward direction. But the sound intensity is identically zero for $\theta = 0°$ or π, since F_{sh} is identically zero along the jet axis. For given x and r, a distribution of sound sources that vary with ϕ as $e^{in\phi}$ is seen by an observer at the jet axis as a collection of sources and equivalent sinks that are at the same distance. Therefore, the sound generated by the sources appear to be completely cancelled by the effective sinks. Thus, along the jet axis all non-axisymmetric wave components produce no far-field sound, leaving the axisymmetric component as the sole contributor.

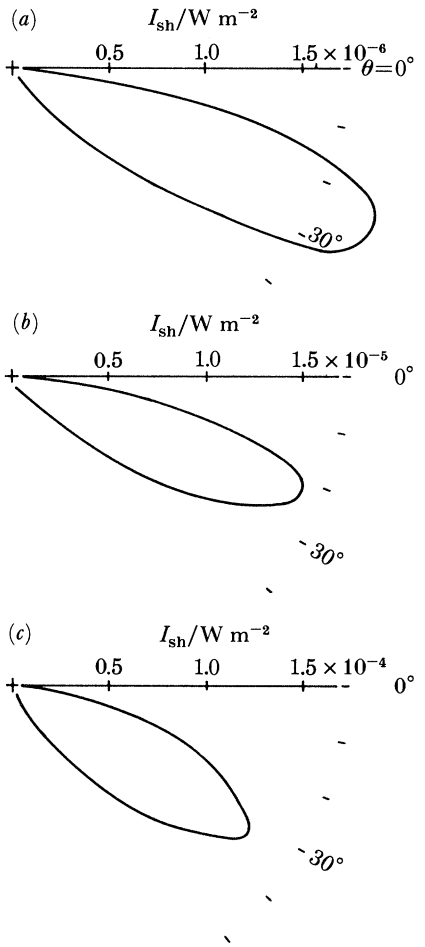

FIGURE 15. Polar distribution of the shear noise intensity I_{sh}(W m^{-2}) for $n = 1$. (*a*) $St = 0.18$; (*b*) $St = 0.30$; (*c*) $St = 0.80$.

If the Strouhal number is large enough (e.g. $St \approx 1.6$) such that the second term in (3.5) is dominant, the directivity pattern would have two dips at $\theta = 63.4°$, $116.6°$ corresponding to the roots of $4\cos^2\theta - \sin^2\theta = 0$. These two dips can be noticed in figure 16 corresponding to $\theta = 60°$ (and $120°$).

As was noted before, at $\theta = 90°$ the aerodynamic sound sources are produced only by V and $\partial V/\partial r$, and this explains the small level of the 90° far-field sound (and the reason why its spectrum is different from other angles) in figure 16. The directivity implied in γ and N and the proportionality of the source term to $\sin 2\theta$ produce a peak emission at $\theta \approx 25°$ at low frequencies, shifting to $\theta \geqslant 30°$ at higher frequencies. The radiation pattern thus resembles

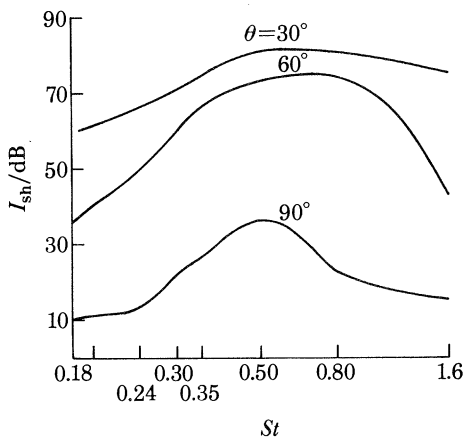

FIGURE 16. Spectra of shear noise intensity I_{sh} referred to 10^{-12} W m^{-2} for $n = 1$.

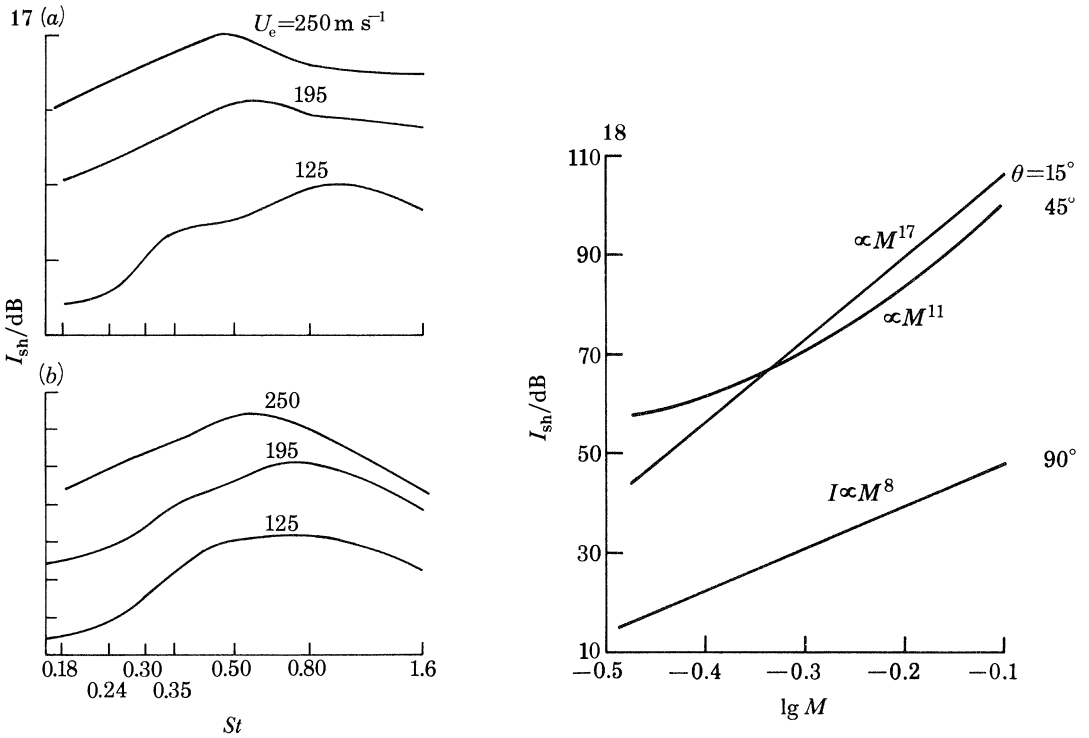

FIGURE 17. The effect of jet exit velocity on the spectra of shear noise for $n = 1$. (*a*) $\theta = 15°$; (*b*) $\theta = 45°$.

FIGURE 18. The dependence of shear noise intensity on jet exit velocity for several emission angles for $n = 1$ and $St = 0.50$.

that of a forward lateral quadrupole. Again, the shift of the peak emission angle here with frequency cannot yet be conclusively compared with observations.

The spectra of the shear noise intensity of the $n = 1$ source component are shown in figure 16 for several values of θ. The spectra exhibit behaviour similar to that for the $n = 0$ mode but peak at higher Strouhal numbers. This shift in the peak Strouhal number can be attributed to the behaviour of $A(x)$ by the following reasoning. The far-field sound depends on the imbalance between the rates of growth and decay of the wave. For the $n = 1$ sources, the rate

of decay increases with Strouhal number faster than it does for the $n = 0$ sources. Thus, the imbalance between the source function's axial rate of growth and rate of decay (see figures 7 and 14) increases with Strouhal number faster for the $n = 1$ than the $n = 0$ mode. Consequently, the peak noise shifts to a higher Strouhal number for the $n = 1$ sources.

The dependence of the shear noise intensity on the jet exit velocity here is similar to that for the $n = 0$ mode as shown in figure 17. The far-field sound level increases with increasing U_e. The dependence of the acoustic intensity on U_e varies with θ, increasing faster with U_e at smaller angles to the jet axis than at higher angles, as shown in figure 18.

(*c*) *Discussion of the relative contribution to the aerodynamic sound field*

We shall here discuss the relative contribution to the aerodynamic sound field on the basis of the results of §§3(*a*) and (*b*). This will lead to an understanding of the spectral behaviour that is essential for comparison with observations in §4.

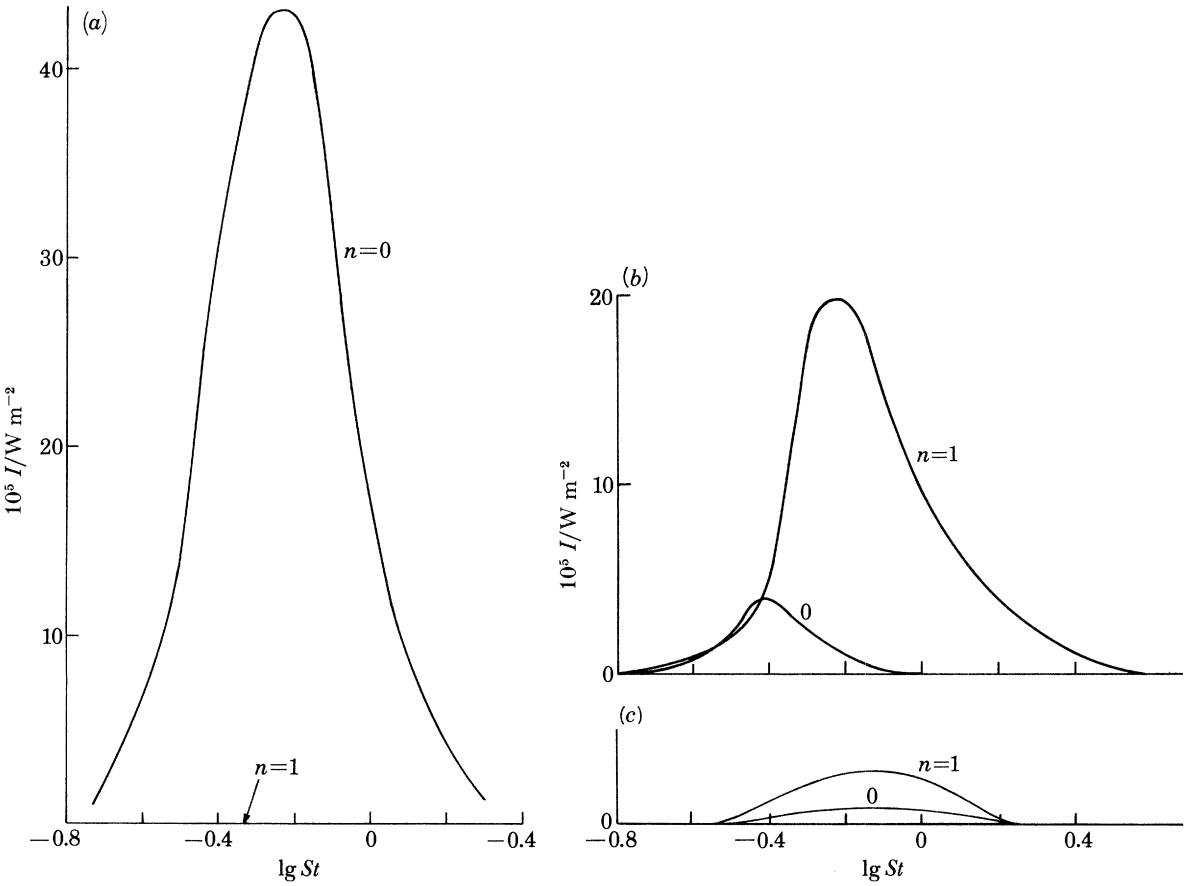

FIGURE 19. Relative contributions to the shear noise intensity. (*a*) $\theta = 0°$; (*b*) $\theta = 30°$; (*c*) $\theta = 60°$.

The $n = 0$ mode shear noise strongly resembles the longitudinal xx-quadrupole in that it contributes predominantly to the intensities along the jet axis. At 90° to the jet axis the contribution of the shear noise is negligible compared with that at small emission angles.

The $n = 1$ mode shear noise, which makes no contribution to the radiation along the jet

axis, somewhat resembles the lateral xr-quadrupole radiation pattern and peaks in the vicinity of $\theta \approx 30°$. The shear noise at 90° is about 4–5 orders of magnitude less than that at $\theta \approx 30°$.

In general, peaking of the $n = 1$ intensities occurs at higher frequencies than that of the $n = 0$ mode. Figure 19 indicates the relative contribution of each azimuthal component at several emission angles against St. At small angles to the jet axis, the $n = 0$ shear noise dominates. As θ increases, the $n = 1$ mode becomes important. The $n = 0$ shear noise occurs dominantly at low Strouhal numbers while the $n = 1$ mode dominates at larger Strouhal numbers. The shear noise of both $n = 0$ and 1 modes are of the same magnitude, though that of the $n = 1$ mode dominates that of the $n = 0$ mode at larger Strouhal numbers. This is entirely in agreement with Yamamoto & Arndt's (1978) deduction from their observations.

For the same initial levels at the nozzle exist for the $n = 0$ and 1 modes the overall shear noise would peak near $\theta \approx 0°$. However, if the initial levels of the $n = 1$ mode were relatively higher, the overall shear noise peak would shift away from the jet axis towards $\theta \approx 30°$. Thus, the shear noise in general peaks between 0° and 30°. The xx-quadrupole nature of shear noise was observationally deduced much earlier by Mollo-Christensen *et al.* (1964), Csanady (1966) and Krishnappa & Csanady (1969).

The higher frequency sound is mainly a result of the $n = 1$ mode. Now figure 2 shows that the $n = 1$ mode within the jet is concentrated in a small region close to the jet exit ($x/d \approx 0$–5), compared with the $n = 0$ mode at the same St. The high frequency sound would thus appear to come from a small region close to the jet exit. For the low frequency sound both $n = 0$ and $n = 1$ modes are important and since the $n = 0$ mode extends over longer range along the jet ($x/d \approx 0$–20) the low frequency sound would seem to be generated over an extended region of the jet. This is entirely consistent with the earlier and recent observations (e.g. Fitzpatrick & Lee 1952; Gerrard 1953; Lassiter & Hubbard 1952; Lush 1971; Ahuja & Bushell 1973).

We have not presented results for the self-noise of both the $n = 0$ and 1 modes because these were found to be more than 20–50 dB lower than the corresponding shear noise. However, it is interesting to note that in general for the $n = 0$ mode the self-noise peaks at a lower St compared with that of the shear noise for forward emission angles and is relatively more omnidirectional. The latter is also true for the $n = 1$ mode self-noise, but radiation peaks at a larger St than the corresponding shear noise.

4. Comparisons with observations

In a real turbulent jet, undoubtedly the composition of large-scale coherent structures encompasses more than just the $n = 0$ and 1 modes discussed in §3. However, Batchelor & Gill (1962) showed that for dynamical instabilities the $n = 1$ mode is unstable and that complete stabilization occurs for modes with large n. Measurements in a round turbulent jet by Michalke & Fuchs (1975) show that the $n = 0$ and 1 modes dominated the pressure fluctuations. They also showed theoretically that the higher order n modes would be inefficient acoustic emitters. In this case, the contribution to the total jet noise can be adequately approximated by the shear and self-noise of the dominant $n = 0$ and 1 modes. In the absence of detailed information on the initial conditions, it is not unreasonable to assume that the initial disturbances at the nozzle exit are sufficiently 'broad band' that the $n = 0$ and 1 modes are likely to be initiated with amplitudes of the same order. It is most likely that the nozzle exit disturbances differ for different experimental set-ups, so that the large-scale structure initial

disturbance level, $|A|_0^2$, differs. However, the correct order of magnitude of the far field sound is achieved by $|A|_0^2 \approx 10^{-5}$, which is close to the nozzle exit measurements of Moore (1977) in natural turbulent jets. The fine-grained turbulence level E_0 also has a profound influence on the development of the large-scale structure and thus its acoustic output.

Another factor in the actual aerodynamic sound measurements that is not easily assessed theoretically is the contribution from the fine-grained turbulence. However, it is not entirely speculative to regard it as of less-efficient emitters and that it would contribute to a nearly isotropic radiation pattern. In this case, spectral variations of the peak radiation and the directivity are predominantly contributed by the large-scale structures. At angles where the large-scale structure contribution is very small, such as at $\theta = 90°$, the noise contribution of the fine-grained turbulence as well as other large-scale azimuthal components, may be relatively crucial and can no longer be considered negligible with respect to the contribution of the $n = 0$ and 1 modes. The meaningful way to compare the present theoretical results,

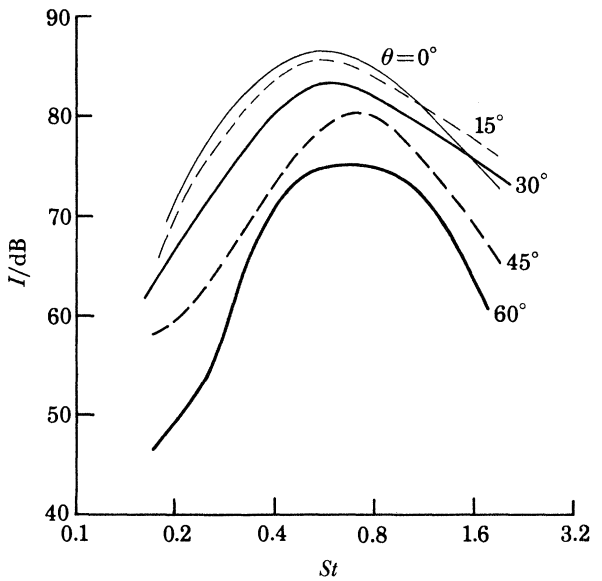

FIGURE 20. Calculated spectra of sound intensity in decibels referred to 10^{-12} W m^{-2} due to coherent structures at various emission angles for $U_e = 195$ m s^{-1}.

which do not include the acoustic contributions from the fine-grained turbulence, with aerodynamic sound measurements from turbulent jets with uncertain $|A|_0^2$ and E_0 is by way of a comparison of the spectral dependence of the angular distribution of *relative* rather than absolute acoustic intensity levels, as has been the practice in aerodynamic sound comparisons.

The acoustic output calculations are obtained for a jet exit velocity of $U_e = 195$ m s^{-1} ($M = 0.565$) and consists of the shear and self-noise contributions from the two modes, $n = 0, 1$. We recall that the large-scale structure source calculations were obtained under the assumption of an incompressible fluid (Mankbadi & Liu 1981), as in §3 with $|A|_0^2 \approx 10^{-5}$, $(\overline{u'^2})^{\frac{1}{2}} \approx 1\%$ and an initial mean flow momentum thickness of about 0.017 the jet nozzle diameter. The observation distance is taken to be 120 jet nozzle diameters.

We show in figure 20 the calculated spectra for emission angles $\theta = 0°$, 15°, 30°, 45°, 60°. We show also in figure 21 the measured spectra of Ahuja & Bushell (1973) and Lush (1971)

for various emission angles, with the horizontal axis re-drawn in terms of Strouhal number to facilitate comparison. The calculated spectra of $\theta = 90°$, 120°, which are not shown, were found to be much smaller compared with observations. The low level of computed sound with respect to observations at larger emission angles is attributed, as before, to the fine-grained turbulence and possibly other azimuthal modes not accounted for in this calculation.

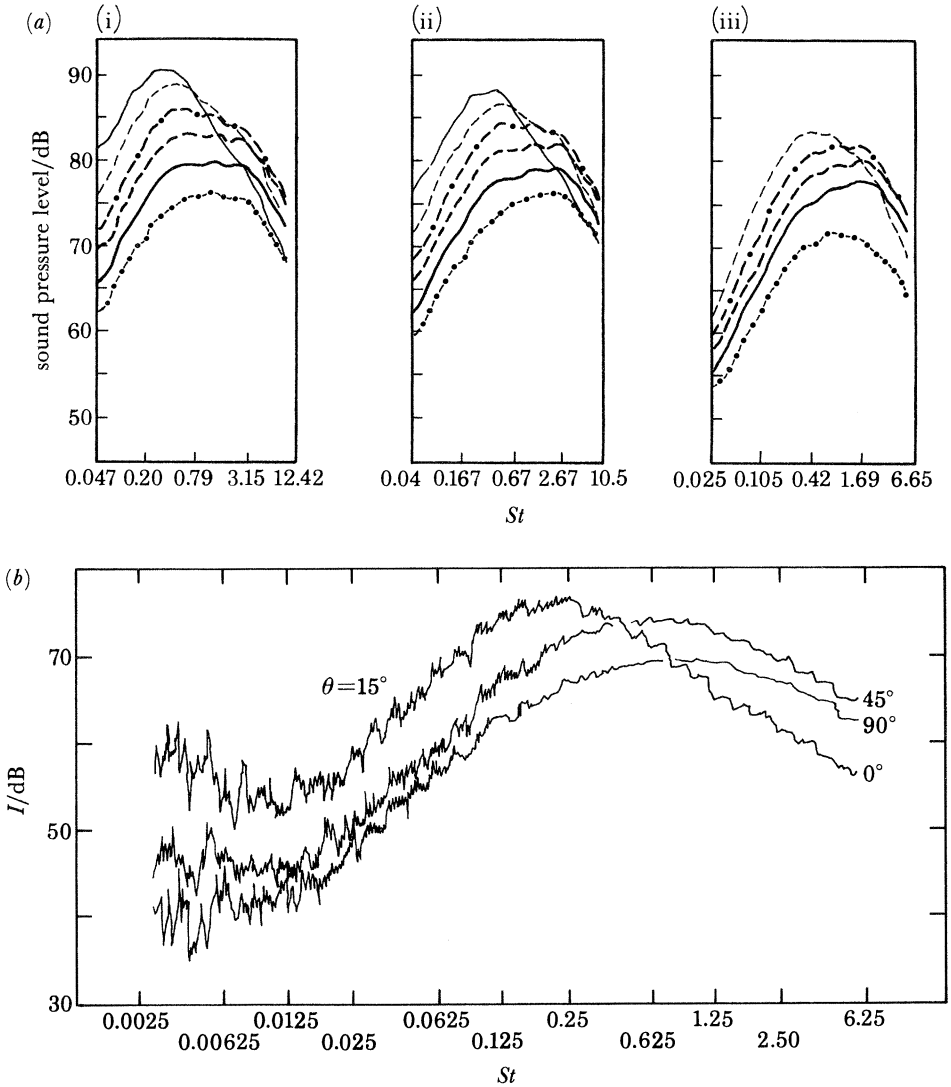

FIGURE 21. Observed $\frac{1}{3}$-octave spectra for various emission angles. (*a*) Ahuja & Bushell (1973), $U_e = 600$ m s^{-1}, $M = 0.53$; ——, $\theta = 20°$; – – –, $\theta = 30°$; —·—, $\theta = 45°$; – – –, $\theta = 60°$; ——, $\theta = 90°$, –•–•–, $\theta = 120°$. (i) $d = 2.84$, $R/d = 25.3$; (ii) $d = 2.4$, $R/d = 30$; (iii) $d = 1.52$, $R/d = 47.4$.(*b*) Lush (1971).

Figure 20 shows that the peak emission moves towards higher Strouhal numbers as the emission angle is increased. This characteristic is similar to the observed spectra of Ahuja & Bushell (1973) as well as those of Lush (1971) in figure 21. The calculated peak Strouhal number is very close to the observed one. The noise level is also close to the observed one except at low emission angles at high frequency where the observed values are less than the computed ones. One can conjecture that the bending of the high frequency sound waves by the jet flow, away

from the jet would account for the relative lower observed frequency content at the smaller emission angles compared with calculations that do not account for such refraction effects explicitly. This is in agreement with Lush's (1971) deduction. Another feature is that in terms of the decibel scale, the calculated spectra is narrower than those observed. The broad-band 'isotropic' turbulence sound, which is not taken into account here, would account for the relatively broader observed spectrum. For instance, the calculated spectra from figure 20 shows an increase of about 13 dB per octave on the low frequency side and a decrease of about 7–11 dB per octave in the high frequency side, a respective deficit from observations (Lush 1971) of about 4–7 dB per octave on either side.

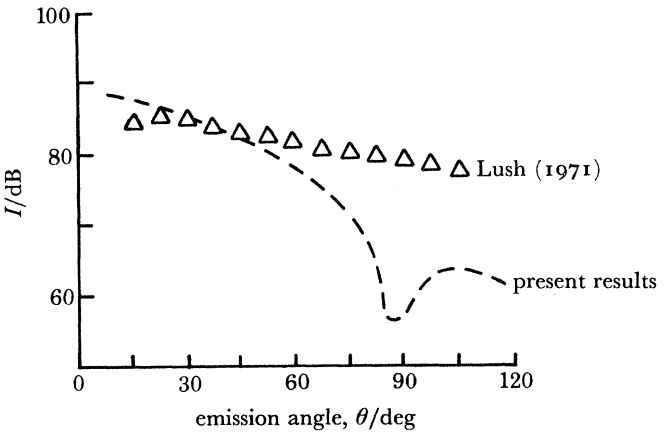

FIGURE 22. Directivity of large-scale coherent structures sound intensity, comparison with Lush (1971) for $U_e = 195$ m s^{-1}.

The contribution to the overall sound at each emission angle is the sum of the contributions under the spectrum (on the linear scale) and this is dominated by the small Strouhal number range surrounding the peak. Such peaks, as well as their shift with emission angle, are attributed here to the large-scale coherent structures. In this case, the overall directivity of aerodynamic sound is represented by the properties of those due to the large-scale structures, as in figure 22 compared with the observation of Lush (1971), shifted for a best fit. The agreement is generally encouraging, however; at small emission angles observed radiation intensities are less than those calculated which may be attributable to the refraction effects in a real jet flow. At larger emission angles the computed intensities are below the observed values; we attribute this deficit to the fine-grained turbulence contribution which was not accounted for here.

The relation between the calculated peak frequency (normalized by the jet diameter and the speed of sound) and the emission angle shown in figure 23*a* and compared with Lush (1971). The corresponding rescaled frequency is shown in figure 23*b*, where $\bar{M}_c$ is an averaged convection Mach number. In general, as already noted in the discussion of the spectra (figure 20), the agreement with observations is reasonably good away from the vicinity of the jet axis. Again, this may be attributable to the acoustic-flow interaction process near the jet axis.

The effect of the jet velocity, U_e, on the noise spectra is shown in figure 24 for $\theta = 15°$. The peak Strouhal number generally decreases with increasing jet velocity but the effect is more pronounced at the smaller emission angles $\theta = 15°$. If the variation of peak Strouhal number with jet velocity is replotted with the peak frequency scaled as $f_p d/a_0 = St_p M$, figure 24 shows that the peak frequency at small emission angles is more or less independent of the

jet exit velocity and is given by $f_p d/a_0 \approx 0.32$. This is in accordance with experimental observations of Lush (1971) and Ahuja & Bushell (1973), which give $f_p d/a_0 \approx 0.2$ at small emission angles. At 45° it is found that decrease of St_p with jet velocity is less pronounced. This is consistent with the experimental observation of Lush (1971) that the peak frequencies of the $\frac{1}{3}$-octave spectra scaled on Strouhal number at emission angles at right angles to the jet. The peak of the calculated 90° spectra cannot be compared with experiment as the coherent structures cannot be considered as the dominant sound source at 90° as discussed earlier.

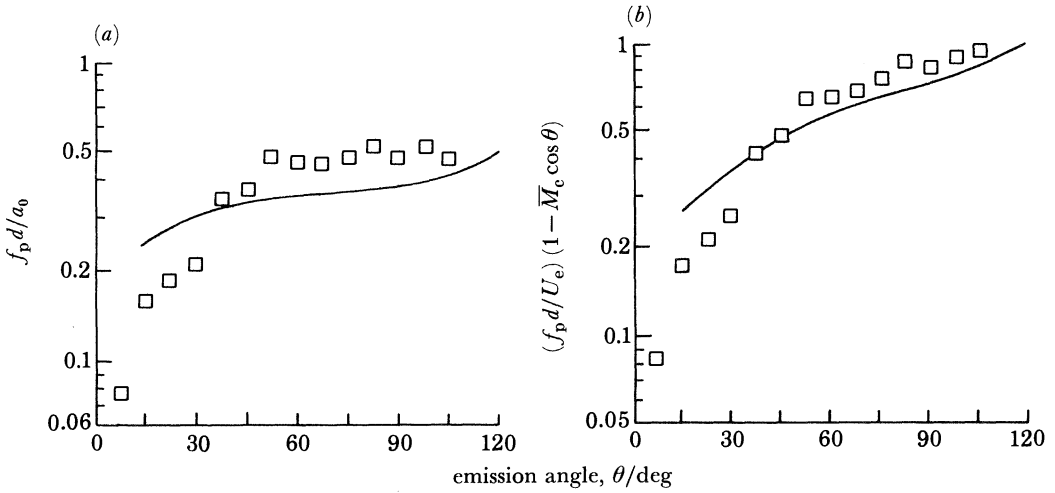

FIGURE 23. Variation of peak frequency with emission angle, comparison with Lush (1971).

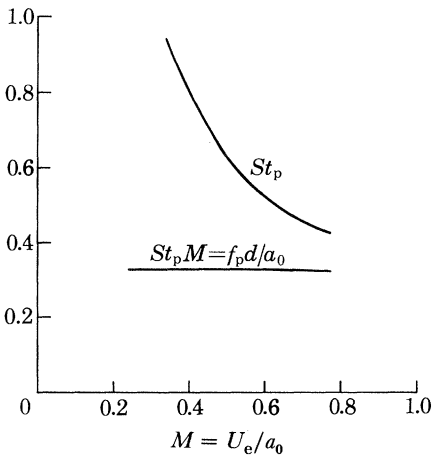

FIGURE 24. Effect of jet exit velocity on the peak frequency near the jet axis, $\theta = 15°$.

The dependency of the total sound intensity on the jet exit velocity is shown in figure 25. At right angles to the jet axis the sound intensity is proportioned to M^8 according to Lighthill (1952) and in agreement with experimental observations. But the calculated 90° noise is about 40 dB (four orders of magnitude) less than the observed values. Therefore, it is not shown in figure 25. The calculated intensity is plotted in absolute scale without readjusting the vertical scale. The calculated intensity dependence on jet velocity, when assumed to be $I \propto M^m$ would give an index that increases from $m = 8$ at $\theta = 90°$ to about $m = 14$ at $\theta = 15°$. The increase of index with emission angle is stronger than that observed. The latter gives an index

as 9 at low emission angles. This could be attributed to the refraction effect which would decrease the sound intensity at low emission angles, and the compressibility effect which was ignored in the source calculations. Compressibility would cause a stabilizing effect as the Mach number increases, leading to reducing the amplification of the coherent structure and hence reducing its sound intensity.

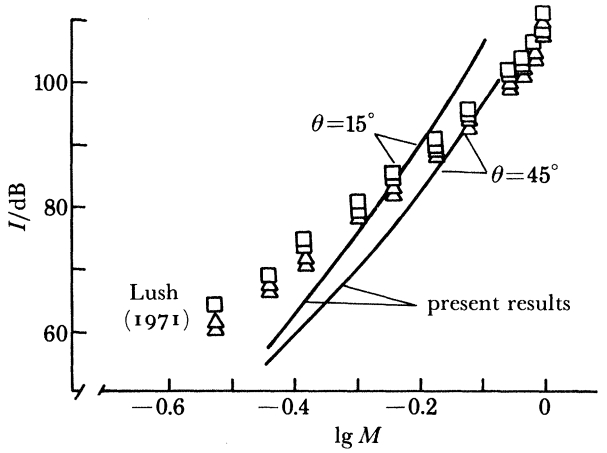

FIGURE 25. Dependence of total sound intensity on jet velocity.

5. FURTHER DISCUSSION

In the present work the dominant aerodynamic sound sources are considered to be the coherent large-scale structures that are inherently present in turbulent jets. The description of the sources is obtained from approximate but dynamically (or energetically) consistent conservation principles. As such, this is to be contrasted with analytically integrable but modelled source distributions (see, for example, Crow 1972; Crighton 1975; Ffowcs Williams & Kempton 1978). The source distribution here consists of the two lowest order azimuthal modes ($n = 0, 1$) over a Strouhal number spectrum relevant to jet noise. The question that naturally arises is what additional features would the inclusion of higher azimuthal modes present. We know, in general, that the $n = 0$ mode radiates effectively as if it were a longitudinal quadrupole and the $n = 1$ mode a lateral quadrupole (but the details depend upon the frequency). Insight to the higher mode behaviour can be gained by comparing approximately the relative features of the $n = 2$ and $n = 1$ modes. To this end, we make use of the same small σ expansion discussed in §3 for Z_n. If we attribute the dominating term in Z_n as that with coefficient involving $\partial U/\partial r$, then $Z_1 \approx \sin 2\theta$ which peaks at 45° and $Z_2 \approx \sin\theta \sin 2\theta$ which peaks at about 55°. These crude estimates are of course modified by the spectrally dependent radial and axial interference functions. However, it can be inferred from the present work and from Michalke & Fuchs (1975) that the peak radiation contributed by higher modes would occur at higher frequencies than the lower-order azimuthal modes. This picture essentially reinforces the notion derived here that Lighthill's (1952) fundamental aerodynamic sound formulation gives rise to a far-field radiation pattern in accordance with the details of observations, provided that the properly-described structure of the sources is accounted for.

Because the downstream development of the coherent structures away from the nozzle lip is necessarily of a non-equilibrium nature and is therefore rather sensitive to the initial

conditions, such as the initial levels of the coherent structure and of the fine-grained turbulence, the mean flow status at the nozzle exit as well as the azimuthal mode and Strouhal number concerned. The set of initial conditions used here for the numerical example is representative of that of natural or weakly forced jets and as such, sets a particular pattern of downstream distribution of, say, the value of the coherent structure amplitude peaks, the location of such peaks, the mean flow spreading rate and the level of fine-grained turbulence. These are by no means universal because, in general, of the non-equilibrium nature of the interactions between the different scales of motion which are necessarily sensitive to initial as well as environmental conditions. From this, we can understand that the observed natural turbulent jets and their far sound field are anything but universal in detail. For instance, the spreading rate of natural turbulent mixing layers is not unique (see the discussion in Alper & Liu 1978) and the spectra of sound from turbulent jets bear a strong qualitative rather than quantitative resemblance to one another (Zaman & Yu 1984). It is precisely because of the sensitivity of the coherent structures to initial and environmental conditions that a variety of methods for their control is discussed by Mankbadi & Liu (1981). For instance, an initially thicker boundary layer weakens the downstream development of the coherent structures. The same purpose is also achieved by increasing the initial levels of the fine-grained turbulence, such as via a fine-meshed screen (Arndt *et al.* 1972; Wei & Niu 1983). An implicit way of controlling the coherent structures comes from an understanding of the energy transfer mechanisms between such structures and the fine-grained turbulence (Mankbadi & Liu 1981; Liu 1981). Forcing a particular mode of the coherent structure that has the most efficient energy transfer rate to the fine-grained turbulence would increase the levels of the 'dissipative' recipient and this in turn would curtail the development of the other components of the large-scale structures much in the same manner as the placing of a series of screens in the jet. The amplification of broadband jet noise by a pure tone excitation has already been demonstrated in the work of Bechert & Pfizenmaier (1975); the reduction of sound radiated by forcing was demonstrated by Moore (1977) and Kibens (1980).

The radiation pattern in the far sound field derived here is entirely reconcilable with the sound sorces in a manner that is fully consistent with observations. This is in no small way due to the physical account given to the spectral dependence of the source development within the turbulent jet. It is thus found that the low-frequency radiation that dominates in the forward direction is attributed to those low-frequency coherent structures that have an extended axial lifespan and whose amplitudes peak further downstream; on the other hand, higher-frequency radiation that points at angles away from the jet axis are primarily attributed to those coherent structures that have shorter axial lifespan with amplitudes that peak closer to the nozzle lip. The present work took into account only the two lowest azimuthal modes. This theoretical picture is in accordance with and essentially summarizes the earlier experimental efforts directed at jet noise source location (Lassiter & Hubbard 1956; Howes *et al.* 1957; Potter & Jones 1968). Though controversial at the time, the measured pressure fluctuations in the near jet noise field are now understood to be a direct consequence of the local activities of the coherent structures (Liu 1974; Merkine & Liu 1975) consistent with the spectrally dependent streamwise activity and lifespan discussed in the present work and in Mankbadi & Liu (1981). The contribution of the present work is seen as that in the observations to have brought more intimately together the mechanism of the causes and the resulting aerodynamic sound field of real turbulent jets.

We have only discussed, from the standpoint of jet noise applications, the problem of a fully turbulent jet. However, in certain instances when the fully turbulent jet conditions are not achieved or desired in the laboratory the questions that need to be raised concerns the mechanisms at work within the transitional jet structure and their effect on the far sound field (Huerre & Crighton 1983; Laufer & Yen 1983). We have strongly emphasized that the coherent structure source distribution, which can be effectively depicted as a line radiator as was done by Crow (1972), generates the far sound field through a net imbalance of quasi-periodic positive and negative contributions under a growing and decaying axial envelope determined through frequency-dependent nonlinear interactions. It has been known for some time (see, for example, Michalke 1971) that the shape distribution of the coherent structures responds to the local profiles of the mean shear flow regardless of whether it is turbulent or laminar; however, the streamwise development of the 'envelope' depends strongly on the nonlinear imbalances between the mechanisms of energy supply and 'dissipation'. In a purely laminar jet the most unstable mode and its harmonics are likely to generate discrete sound in the absence of strong broad-band disturbances. The coherent structures persist much further downstream owing to the much less efficient dissipative mechanism of a laminar flow. Inherent in real flows, however, are the possible presence of weak broad-band fine-grained disturbances. They become strained and amplified by the developing coherent large-scale structure resulting in the latter's earlier demise (Liu & Merkine 1976; Alper & Liu 1978; Mankbadi & Liu 1981). This process is necessarily Reynolds-number dependent, since the rate of energy extracted by the fine-grained disturbances from the coherent structure (and from the mean flow) must overcome the rate of viscous dissipation. Thus, there is a Reynolds number for the same initial and environmental conditions, below which the broad-band fine-grained disturbances, even if artificially generated, would remain inactive. This is, of course, the physical interpretation of the so-called 'critical Reynolds number' for the fine-grained turbulence to develop, which again is dependent upon the initial and environmental conditions and by no means necessarily universal. For sufficiently large Reynolds numbers for transition to take place in the noise-producing region of the jet, then the early decay of the coherent structure would have a noticeable influence on the far sound field. A 'sudden' decay of the coherent structure, whether artificially placed in the computations (Michalke 1969) or caused by the transition process in a real jet, is to the far sound field effectively the placing of a dipole at the location of the 'cut-off'. The flow structure in transitional jets is much more sensitive to initial and environmental conditions than a fully turbulent jet issuing from nozzles with turbulent boundary layers. As such, the careful study of the structural aspect of the transitional jet itself must necessarily be made an integral part of the quantitative study and understanding of its aerodynamic sound field. The present framework for the source description also provides a basis for the study of coherent structures in a laminar flow undergoing dissipation by weak fine-grained turbulence such as in a transitional jet, thereby providing the proper 'switch-on' and 'cut-off' processes for the aerodynamic sound problem. The details, however, remain to be explored in the light of similar experiments.

Aspects of this work were presented at the 35th Annual Meeting of the Division of Fluid Dynamics, American Physical Society (Liu 1982), at the 25th British Theoretical Mechanics Colloquium (Liu & Mankbadi 1983) and at the Symposium on Recent Advances in Aeronautics and Aeroacoustics, Palo Alto (Liu 1983). This work is partly supported by the Fluid

PHILOSOPHICAL TRANSACTIONS OF THE ROYAL SOCIETY A MATHEMATICAL, PHYSICAL & ENGINEERING SCIENCES

Mechanics Program, National Science Foundation through grant NSF MEA78-22127 and the National Aeronautics and Space Administration, Langley Research Center through grant NAG-1-379.

References

Ahuja, K. K. & Bushell, K. W. 1973 An experimental study of subsonic jet noise and comparison with theory. *J. Sound Vib.* **30**, 317.

Alper, A. & Liu, J. T. C. 1978 On the interactions between large-scale structure and fine-grained turbulence in a free shear flow. II. The development of spatial interactions in the mean. *Proc. R. Soc. Lond.* A **359**, 497.

Armstrong, R. R., Michalke, A. & Fuchs, H. V. 1977 Coherent structures in jet turbulence and noise. *AIAA Jl* **15**, 1011.

Arndt, R. E. A., Tran, N. & Barefoot, G. 1972 Turbulence and acoustic characteristics of screen perturbed jets. *AIAA* paper no. 72–644.

Batchelor, G. K. & Gill, A. E. 1962 Analysis of the stability of axisymmetric jets. *J. Fluid Mech.* **14**, 529.

Bechert, D. & Pfizenmaier, E. 1975 On the amplification of broad-band jet noise by pure tone excitation. *J. Sound Vib.* **43**, 581.

Bishop, K. A., Ffowcs Williams, J. E. & Smith, W. 1971 On the noise sources of the unsuppressed high-speed jet. *J. Fluid Mech.* **50**, 21.

Brown, G. L. & Roshko, A. 1974 On density effects and large-scale structure in turbulent mixing layers. *J. Fluid Mech.* **64**, 775.

Crow, S. C. 1972 Acoustic gain of a turbulent jet. *Div. Fluid Dynamics Meeting, Am. phys. Soc., Boulder, Colorado.* Paper IE.6.

Crighton, D. G. 1975 Basic principles of aerodynamic noise generation. *Prog. aerospace Sci.* **16**, 31.

Csanady, G. T. 1966 The effect of mean velocity on jet noise. *J. Fluid Mech.* **26**, 183.

Dimotakis, P. E. & Brown, G. L. 1976 Large structure dynamics and entrainment in the mixing layer at high Reynolds numbers. *J. Fluid Mech.* **78**, 535.

Dowling, A. P., Ffowcs Williams, J. E. & Goldstein, M. E. 1978 Sound production in a moving stream. *Phil. Trans. R. Soc. Lond.* A **288**, 321.

Ffowcs Williams, J. E. & Kempton, A. J. 1978 The noise from the large-scale structure of a jet. *J. Fluid Mech.* **84**, 673.

Fitzpatrick, H. M. & Lee, R. 1952 Measurement of the noise radiated by subsonic air jets. *Rep. David W. Taylor Model Basin*, Washington, no. 835.

Gatski, T. B. & Liu, J. T. C. 1980 On the interactions between large-scale structure and fine-grained turbulence in a free shear flow. III. A numerical solution. *Phil. Trans. R. Soc. Lond.* A **293**, 473.

Gerrard, J. H. 1953 An investigation of the noise produced by a subsonic air jet. Ph.D. thesis, University of Manchester.

Gerrard, J. H. 1956 An investigation of noise produced by a subsonic air jet. *J. aeronaut. Sci.* **23**, 855.

Ho, C. M. & Huang, L. 1982 Subharmonics and vortex merging in mixing layers. *J. Fluid Mech.* **119**, 443.

Howes, W. L., Callaghan, E. E., Coles, W. D. & Mull, H. R. 1957 Near noise field of a jet engine exhaust. *NACA Rep.*, Washington, no. 1338.

Huerre, P. & Crighton, D. G. 1983 Sound generation by instability waves in a low Mach number jet. *AIAA* paper no. 83-0661.

Kibens, V. 1980 Discrete noise spectrum generated by an acoustically excited jet. *AIAA Jl* **18**, 434.

Krishnappa, G. & Csanady, G. T. 1969 An experimental investigation of the composition of jet noise. *J. Fluid Mech.* **37**, 149.

Lassiter, L. W. & Hubbard, H. H. 1952 Experimental studies of noise from subsonic jets in still air. *Tech. Notes natn. advis. Comm. Aeronaut., Wash.*, no. 2757.

Lassiter, L. W. & Hubbard, H. H. 1956 The near noise field of static jets and some model studies of devices for noise reduction. *NACA Rep.*, Washington, no. 1261.

Laufer, J. & Yen, T. C. 1983 Noise generation by a low Mach number jet. *J. Fluid Mech.* **134**, 1.

Lighthill, M. J. 1952 On sound generated aerodynamically. I. General theory. *Proc. R. Soc. Lond.* A **211**, 564.

Lighthill, M. J. 1954 On sound generated aerodynamically. II. Turbulence as a source of sound. *Proc. R. Soc. Lond.* A **222**, 1.

Lighthill, M. J. 1962 Sound generated aerodynamically (The Bakerian Lecture, 1961). *Proc. R. Soc. Lond.* A **267**, 147.

Lighthill, M. J. 1963 Jet Noise. *AIAA Jl* **1**, 1507.

Lilley, G. M. 1971 Sound generation in shear flow turbulence. *Fluid Dynamic Trans.* (Warszawa) **6**, 405.

Liu, J. T. C. 1971 On eddy Mach wave radiation source mechanism in the jet noise problem. *AIAA paper*, no. 71–150.

Liu, J. T. C. 1974 Developing large-scale wavelike eddies and the near jet noise field. *J. Fluid Mech.* **62**, 437.

Liu, J. T. C. 1977 The large-scale coherent structures in turbulent free shear flows and their far aerodynamic sound field. *Workshop on Flow Noise Generation by Large Scale Structures*, 29–30 March. National Aeronautics and Space Administration, Langley Research Center.

PHILOSOPHICAL TRANSACTIONS OF THE ROYAL SOCIETY A MATHEMATICAL, PHYSICAL & ENGINEERING SCIENCES

Liu, J. T. C. 1981 Interactions between large-scale coherent structures and fine-grained turbulence in free shear flows. In *Transition and turbulence* (ed. R. E. Meyer), pp. 167–213. Academic Press.

Liu, J. T. C. 1982 Panel discussion: current approaches to jet noise. *Bull. Am. phys. Soc.* **27**, 1191.

Liu, J. T. C. 1983 Large-scale coherent structures in free turbulent flows and their aerodynamic sound. *Int. Symp. Recent Advances in Aeronautics and Aeroacoustics*, 22–26 August 1983, Palo Alto.

Liu, J. T. C., Alper, A. & Mankbadi, R. 1977 The large-scale organized structures in free turbulent shear flow and its radiation properties. In *Structure and mechanisms of turbulence*, vol. II (ed. E. Wygnanski), pp. 202–218. Berlin: Springer-Verlag.

Liu, J. T. C. & Mankbadi, R. 1983 Sound generated aerodynamically revisited – coherent structures in a turbulent jet as a source of sound. *25th British Theoretical Mechanics Colloquium*, 21–25 March 1983, Manchester.

Liu, J. T. C. & Merkine, L. 1976 On the interactions between large-scale structure and fine-grained turbulence in a free shear flow. I. The development of temporal interactions in the mean. *Proc. R. Soc. Lond.* A **352**, 213.

Liu, J. T. C. & Nikitopoulos, D. E. 1982 Mode interactions in developing shear flows. *Bull. Am. phys. Soc.* **27**, 1192.

Lush, P. A. 1971 Measurements of subsonic jet noise and comparison with theory. *J. Fluid Mech.* **46**, 477.

Mankbadi, R. & Liu, J. T. C. 1981 A study of the interactions between large-scale coherent structures and fine-grained turbulence in a round jet. *Phil. Trans. R. Soc. Lond.* A **298**, 541.

Merkine, L. & Liu, J. T. C. 1975 On the development of noise-producing large-scale wavelike eddies in a plane turbulent jet. *J. Fluid Mech.* **70**, 353.

Michalke, A. 1969 Sound generation by amplified disturbances in free shear layers. *Deutsche Luft und Raumfahrt*, rep. no. 69–90. (English Transl. *Brown University, Division of Engineering* by E. Morse.)

Michalke, A. 1971 Instabilität eines kompressiblen runden Freistrahls unter Berücksichtigung des Einflusses der Strahlgrenzschichtdicke. *Z. Flugwiss.* **19**, 319.

Michalke, A. & Fuchs, H. V. 1975 On turbulence and noise of an axisymmetric shear flow. *J. Fluid Mech.* **70**, 179.

Mollo-Christensen, E. 1960 Some aspects of free-shear-layer instability and sound emission. *N.A.T.O.–A.G.A.R.D.* rep. no. 260.

Mollo-Christensen, E. 1967 Jet noise and shear flow instability seen from an experimenter's viewpoint. *Trans. A.S.M.E. J. appl. Mech.* **E89**, 1.

Mollo-Christensen, E., Koplin, M. A. & Martuccelli, J. R. 1964 Experiments on jet flows and jet noise, far field spectra and directivity patterns. *J. Fluid Mech.* **18**, 285.

Moore, C. J. 1977 The role of shear-layer instability waves in jet exhaust noise. *J. Fluid Mech.* **80**, 321.

Pao, S. P. 1973 Aerodynamic noise emission from turbulent shear layers. *J. Fluid Mech.* **59**, 451.

Phillips, O. M. 1960 On the generation of sound by supersonic turbulent shear layers. *J. Fluid Mech.* **9**, 1.

Potter, R. C. & Jones, J. H. 1968 An experiment to locate the acoustic sources in a high speed jet exhaust stream. *Wyle Lab. Res. Staff* Rep. WR 68-4.

Ribner, H. S. 1964 The generation of sound by turbulent jets. *Adv. appl. Mech.* **8**, 103.

Ribner, H. S. 1977 On the role of the shear term in jet noise. *J. Sound Vib.* **52**, 121.

Roshko, A. 1976 Structure of turbulent shear flows: A new look. *AIAA Jl* **14**, 1349.

Wei, Z. L. & Niu, Z. N. 1983 The disturbances affect Brown–Roshko structures in plane mixing layer. In *Structure of complex turbulent shear flow-IUTAM Symposium Marseille 1982*, pp. 137–145, (ed. R. Dumas & L. Fulachier). Berlin: Springer-Verlag.

Westley, R. & Lilley, G. M. 1952 An investigation of the noise field from a small jet and methods for its reduction. *Rep. Coll. Aero. Cranfield* no. 53. Also *A.R.C. Rep* no. 14719.

Williams, D. R. & Hama, F. R. 1980 Streaklines in a shear layer perturbed by two waves. *Physics Fluids* **23**, 442.

Winant, C. D. & Browand, F. K. 1974 Vortex pairing: The mechanism of turbulent mixing-layer growth at moderate Reynolds number. *J. Fluid Mech.* **63**, 237.

Yamamoto, K. & Arndt, R. E. A. 1978 On an acoustic field generated by subsonic jets at low Reynolds numbers. *Univ. of Minnesota St Anthony Falls Hydraulic Laboratory*, Project Rep. no. 170.

Zaman, K. B. M. Q. & Yu, J. C. 1984 Power spectral density of subsonic jet noise. *J. Sound Vib.* (In the press.)

PHILOSOPHICAL TRANSACTIONS OF THE ROYAL SOCIETY A MATHEMATICAL, PHYSICAL & ENGINEERING SCIENCES